Isospin-Forbidden Particle Decays of $T = \frac{3}{2}$ Levels in Mirror Nuclei*

E. G. Adelberger†
California Institute of Technology and Princeton University

and

A. B. McDonald‡
A. E. C. L. Chalk River Nuclear Laboratories, and California Institute of Technology

and

C. L. Cocke,§ C. N. Davids,¶ A. P. Shukla,|| H. B. Mak, and D. Ashery**
California Institute of Technology, Pasadena, California
(Received 9 October 1972)

Absolute branching ratios for the isospin-forbidden particle decays of the lowest $T=\frac{3}{2}$ levels of ^{13}C, ^{13}N, ^{17}O, and ^{17}F have been measured by populating the levels in (^{3}He, p), (^{3}He, α), or (^{3}He, n) reactions and observing the resulting decay products in coincidence. Branching ratios of 0.070 ± 0.018, 0.261 ± 0.030, and 0.026 ± 0.018 (0.236 ± 0.012, 0.150 ± 0.010, 0.053 ± 0.015) were determined for the neutron (proton) decays of the 15.1-MeV, $T=\frac{3}{2}$ level of ^{13}C(^{13}N) to the ground state and first two excited states of ^{12}C, respectively. Branching ratios of 0.91 ± 0.15 and 0.05 ± 0.02 (0.088 ± 0.016, 0.23 ± 0.05) were determined for the neutron (proton) decays of the 11.08-(11.20-) MeV, $T=\frac{3}{2}$ level of ^{17}O(^{17}F) to the ground state and unresolved 6.05- and 6.13-MeV excited states of ^{16}O, respectively. The α-decay branching ratios of the 15.1-MeV, $T=\frac{3}{2}$ level of ^{13}N to the ground state and first two excited states of ^{9}B were determined to be 0.049 ± 0.027, 0.039 ± 0.039, and 0.072 ± 0.045, respectively. Possible origins of the large asymmetries observed in the nucleon decays of these analog levels are discussed. The value obtained for Γ_{p_0}/Γ for the lowest $T=\frac{3}{2}$ level of ^{13}N may be combined with ^{13}C(e,e') and ^{12}C-(p,γ)^{13}N measurements to determine the ratio $\Gamma_\gamma^{M1}(^{13}\mathrm{C})/\Gamma_\gamma^{M1}(^{13}\mathrm{N}) = 1.0 \pm 0.2$ for γ decay to the ground state. This places an upper limit on the isotensor transition matrix element at 7% of the isovector matrix element.

1. INTRODUCTION

One of the more intriguing ideas in nuclear physics is the suggestion that the isospin impurities observed in complex nuclei may be useful in understanding the charge dependence of the internucleon force itself.[1] That the exploitation of this suggestion has not been entirely successful is due in part to the scarcity of sufficiently detailed experimental information on the size and form of these impurities. Let us briefly review the experimental evidence upon which our knowledge of isospin admixtures is based. Isospin-impurity amplitudes are obtained primarily from three sources:

(1) β-decay matrix elements[2];
(2) Electromagnetic (E.M.) selection rules (especially for $E1$ transitions in self-conjugate nuclei[3,4]);
(3) Comparison of isospin-allowed and isospin-forbidden reaction rates.[5-7]

Because of the particularly simple form of the operator for pure Fermi β decays, the transition strengths between $J^\pi = 0^+$ analog states can be predicted with great precision. Hence the strength of an isospin-forbidden transition directly measures the admixture of the analog of the initial (or final) state into the final (or initial) state. Charge-dependent matrix elements[2] obtained from such measurements vary greatly but are on the order of 10 keV. Occasionally the strength of a superallowed Fermi transition is used to set a limit upon the isospin purity of a nucleon state. For instance, from the strength of ^{17}Ne β^+ decay to the lowest $T=\frac{3}{2}$ level of ^{17}F, the isospin purity of the ^{17}F state is found to be $\geq 95\%$.[8]

Isospin-impurity amplitudes derived from isospin-forbidden E.M. transition rates are subject to larger uncertainties than those extracted from β decays. Consider, as an example, the selection rule on $E1$ transitions in self-conjugate nuclei. In the light nuclei ($A \leq 40$), the isospin-forbidden transitions are typically only a factor of 10 weaker than the allowed transitions.[9] One might think that this implied a typical isospin-impurity amplitude of ~30%. However, the allowed $E1$ transitions are themselves very weak, typically 0.002 Weisskopf units (W.u.),[9] since most of the $E1$ strength resides in the giant dipole resonance. In the absence of a detailed theory of the mechanism

of isospin admixtures, it is difficult to convert this factor of 10 inhibition into an impurity amplitude. However, if we make the assumption that the "operative" impurity in these dipole transitions is dominated by an admixture from the giant dipole resonance, then one obtains charge-dependent matrix elements for light nuclei of ~100 keV, which correspond to isospin-impurity *amplitudes* of ~1%. It is reasonable that the average strength of matrix elements inferred from E.M. transitions (100 keV) should be larger than that deduced from β decays (10 keV). In the case of $E1$ decays the charge-dependent interaction connects states with a similar particle-hole structure, while for the pure Fermi β decays, the relevant 0^+ states will, in general, have quite different structures. In principle, isospin-impurity amplitudes are also obtainable from violations of the selection rule that in E.M. transitions $\Delta T = 0$ or ± 1. As yet, however, no such transitions have been observed and the experimental upper limits[10] on transitions where the isospin changes by two units are still roughly a factor of 4 greater than the expected rate due to isospin admixtures in the $T = 2$ state.

For example, in Ref. 10, the $E2$ transition between the 15.4-MeV $T = 2$ state in ^{24}Mg and the 1.37-MeV 2^+ $T = 0$ state is found to have $\Gamma_\gamma < 40$ meV. The width expected from isospin admixtures may be estimated by mixing the ground state into the $T = 2$ state. Assuming that the charge-dependent matrix element connecting these states is 100 keV, and using the known $BE2$ for the 1.37 MeV → ground-state transition, we find a strength of $\Gamma_\gamma = 11$ meV for the 15.4-MeV → 1.37-MeV transition.

Studies of isospin-forbidden particle reactions have, in general, contributed only modestly toward our quantitative understanding of isospin impurities, largely because the strong interaction transition operator is not well understood. Since one cannot reliably calculate the transition rate of an isospin-allowed particle transition, it is difficult to infer impurity amplitudes from measured reaction rates. Nevertheless, impurity amplitudes are frequently deduced by assuming some average strength for the unknown rate. In spite of these limitations, the particle reactions have produced some important and unexpected results. Recent studies of the isospin-forbidden particle decays, such as the present study of the decays of $T = \frac{3}{2}$ levels in $A = 13$ and $A = 17$ and the work of McGrath *et al.*[11] on decays of $2s$-$1d$ shell $T = 2$ states, have revealed the first details of the *form* as well as *size* of isospin impurities.

It should be noted that in our discussion of isospin impurities we have almost always referred to the *operative* rather than the *total* impurity. For example, the impurity determined from an isospin-forbidden β-decay rate is only that fraction of the impurity due to the admixture of a single state, and in the study of isospin-forbidden $E1$ transitions one is sensitive only to that portion of the impurity which has a strong $E1$ strength.

Let us consider in a general way the symmetry properties of isospin impurities. A charge-dependent two-body interaction between $T = \frac{1}{2}$ nucleons may be written in the form $V_{ij} = A + B(\vec{t}^i \cdot \vec{t}^j) + C(t_3^i + t_3^j) + D(t_3^i t_3^j)$ where A, B, C, and D are functions of the space and spin coordinates of particles i and j and $\vec{t}^i$ and t_3^i refer to the isospin vector and third component of the isospin vector of the ith particle. This interaction can be decomposed into isoscalar, isovector, and isotensor components. The first two terms are pure isoscalar, the third pure isovector, and the fourth is a mixture of isoscalar and isotensor. The isotensor term violates charge independence but preserves charge symmetry. The isovector term violates both charge independence and charge symmetry.

The *diagonal* charge-dependent matrix elements, which are presumably dominated by the Coulomb force, are well known from experimentally determined isobaric displacement energies.[12] From these energies it is found that isovector energies are much larger than isotensor energies. For example, in mass 16 the vector energy is ~50 times greater than the tensor energy and this ratio increases with increasing mass. Apparently the diagonal charge-dependent matrix elements are fairly well understood. Recent model-dependent[13,14] and phenomenological[12,15] calculations reproduce the observed displacement energies to accuracies of 50 keV or better.

Much less, of course, is known about the *off-diagonal* charge-dependent matrix elements, since the relevant experimental data (summarized above) are quite sparse. It is often assumed[16-18] that for the off-diagonal elements, as well as for the diagonal elements, the isotensor terms are much smaller than the isovector terms. Calculations of isospin impurities which employ a simple model of nucleons moving in an average Coulomb field necessarily neglect isotensor mixing as the Coulomb force is represented by a one-body operator. Until quite recently there was no compelling reason for considering isotensor mixing, since most of the measured transition speeds were not sensitive to isotensor impurites. However, the rates of isospin-forbidden particle decays of $T = \frac{3}{2}$ and $T = 2$ states are sensitive to isotensor mixing, and have provided strong evidence that, in several cases at least, it is comparable with, and sometimes exceeds, the isovector mixing. Some possi-

ble explanations for this unexpected behavior will be discussed below.

In the present work we have determined branching ratios for isospin-forbidden proton decays of the lowest $T=\frac{3}{2}$ levels of ^{13}N and ^{17}F, neutron decays of the lowest $T=\frac{3}{2}$ levels of ^{13}C and ^{17}O, and α-particle decays of the lowest $T=\frac{3}{2}$ level of ^{13}N. It is our hope that comparisons of experimentally determined isospin-nonconserving particle widths with those calculated from the Coulomb interaction plus a charge-dependent nuclear interaction will eventually prove useful in understanding the charge dependence of the nuclear force. This charge dependence presumably arises from more subtle E.M. effects such as mass differences between the charged and neutral mesons and radiative corrections to the meson-nucleon coupling constants.[19]

In the case of the ^{13}N proton decays, there is an additional justification for the measurement. The absolute radiative width of the lowest $T=\frac{3}{2}$ state can be obtained by combining our measurement of Γ_{p_0}/Γ with the value for $\Gamma_{p_0}\Gamma_{\gamma_0}/\Gamma$ deduced from a study of the ^{12}C(p,γ_0) reaction.[20] This width can then be compared with the analogous width in ^{13}C which has been measured with high precision in inelastic electron scattering.[21,22] These charge symmetric $\Delta T=1$ γ transitions in ^{13}N and ^{13}C should have identical widths, if the levels are truly analogs and the E.M. field contains only isoscalar and isovector components.[4] This selection rule can be accurately tested at present in only one case: mass 13. An accurate test of this rule is especially interesting, since evidence for isotensor E.M. currents has recently been deduced from photoproduction of pions in the region of the lowest $J^\pi=\frac{3}{2}^+$, $T=\frac{3}{2}$ resonance.[23,24] If such currents did exist, then, at some level of accuracy, charge-symmetric $\Delta T=1$ γ-ray transitions should exhibit a charge asymmetry (see Ref. 25). The effect is expected to be quite small in nuclei since "$T=2$" currents cannot couple to single nucleons. We have therefore attempted to measure Γ_{p_0}/Γ for ^{13}N with the greatest possible precision. The resultant value for the ratio of radiative widths in ^{13}C and ^{13}N constitutes the most precise test yet performed on the equality of charge-symmetric $\Delta T=1$ transitions in nuclei. Within the experimental uncertainties no departure from charge symmetry is observed, although the errors are not small enough to place a stringent limit on the presence of isotensor currents.

In Secs. 2 and 3 below, the measurements of the particle decay of the lowest $T=\frac{3}{2}$ levels of mass 13 and 17 nuclei are described. Measurements of known branching ratios which verified the accuracy of the experimental method are described in Sec. 4 and the results are discussed in Sec. 5. An Appendix contains a description of the kinematics of the reactions and the angular correlations of the decay products.

2. BRANCHING RATIO MEASUREMENTS FOR MASS 13

A. Proton Decays of the 15.07-MeV $T=\frac{3}{2}$ Level of ^{13}N

The lowest $T=\frac{3}{2}$ level of ^{13}N has an excitation energy of 15.066 ± 0.004 MeV,[26] a width of ~0.9 keV keV,[27,28] and $J^\pi=\frac{3}{2}^-$.[29,27] We have studied the isospin-forbidden proton decay of this state by forming it in the ^{11}B(^{3}He, n) reaction at $E(^3\text{He})=7.0$ MeV, which populates the 15.07-MeV state with high selectivity.[29] Branching ratios were obtained by detecting decay protons in coincidence with neutrons from the (^{3}He, n) reaction populating the $T=\frac{3}{2}$ state. The neutrons were detected at 0° to align the recoiling ^{13}N nuclei and also to maximize the counting rate, since the neutron angular distribution[29] peaks at 0°.

The experimental apparatus is shown in Fig. 1. The neutron detector was a heavily shielded 5.0-cm-thick by 12.7-cm-diam plastic scintillator coupled to an XP1040 photomultiplier. This detector is used with the California Institute of Technology (CIT) pulsed-beam time-of-flight neutron spectrometer and has been described elsewhere.[30]

The target-to-neutron detector distance used was 1.5 m. Protons were detected by two silicon surface-barrier detectors mounted one behind the other in a 28-cm-diam aluminum scattering chamber with a wall thickness of 0.32 cm. A 50-mg/cm^2 mica foil was placed before the front detector to stop the elastically scattered ^{3}He ions. The detectors consisted of a 1000-μm totally depleted detector followed by a 1000-μm partially depleted detector, both having an active area of 300 mm^2. The totally depleted detector provided good time information for the protons of interest in the n-p coincidence experiment, and the sum of the two detectors provided sufficient thickness to stop the protons from the ^{11}B(^{3}He, p)^{13}C(0.0) reaction. This latter reaction provided an accurate monitor of beam-target interactions as it produced the most energetic peak in the charged-particle spectrum and was clearly resolved. A short dead-time scaler was used to monitor this peak.

The solid angle of the detectors was defined by a circular collimator, 1.59 cm in diam, which was placed 7.39 cm from the target. The ^{3}He beam passed through two 0.16-cm circular tantalum collimators before striking the target and its size and position were accurately measured by allowing it to burn a piece of paper placed in the

target location. In this way a solid angle of 36 msr was determined to ±1% at all angles used.

The targets were 75-$\mu g/cm^2$ self-supporting boron targets enriched to 98.6% in ^{11}B. The beam passed through the targets and was stopped on a small Faraday cup located within the chamber. To determine branching ratios for proton decay, two spectra were obtained at each angle with identical geometry for the proton and neutron detectors. First, a "singles" neutron time-of-flight spectrum was obtained by using a pulsed beam, deriving the start pulses for a time-to-amplitude converter (TAC) from the neutron detector and the stop pulses from the beam-pulsing apparatus. From this spectrum the total population of the ^{13}N ($T=\frac{3}{2}$) level could be determined relative to the ^{13}C (0.0) monitor. A neutron-proton coincidence spectrum was then obtained, using the continuous beam of the tandem accelerator in order to maximize the real-to-random counting ratio. Neutron flight times were determined from the time difference between associated pulses from the neutron and proton detectors, which provided start and stop pulses, respectively, for a TAC. The timing signal from the silicon surface-barrier detector was derived from a time-pickoff unit patterned after one described by Sherman, Roddick, and Metz.[31] The time resolution for p-γ coincidences was better than 1.5 nsec so that the time resolution for the 1-MeV neutrons of interest was prodominantly determined by the 5-cm thickness of the plastic scintillator which contributed 3.5 nsec. As the beam-pulse length and electronic contributions to the time resolution in the singles spectrum were also small compared with 3.5 nsec, the line shape for the $T=\frac{3}{2}$ level was similar in the singles and coincidence spectra. This increased the accuracy with which their ratio could be determined.

The triggering efficiency of the time-pickoff unit on the surface-barrier detector was repeatedly tested to make sure that it was 100% for the decays of interest. The neutron counter was entirely surrounded by a copper shield to prevent pulses in the photomultiplier from triggering the time-pickoff unit.

The neutron-detection efficiency was defined as described in Ref. 30 by setting a discrimination level at a point equivalent to $\frac{1}{8}$ of the midpoint of the Compton edge of the 662-keV γ rays from a ^{137}Cs source. This level was checked regularly to ensure a constant neutron-detection efficiency.

A block diagram of the electronic circuits is shown in Fig. 2. Two-dimensional spectra of proton energy versus neutron time of flight were accumulated as a 64×64-channel array. A typical spectrum is shown in Fig. 3. The form of this spectrum is described in detail in the Appendix.

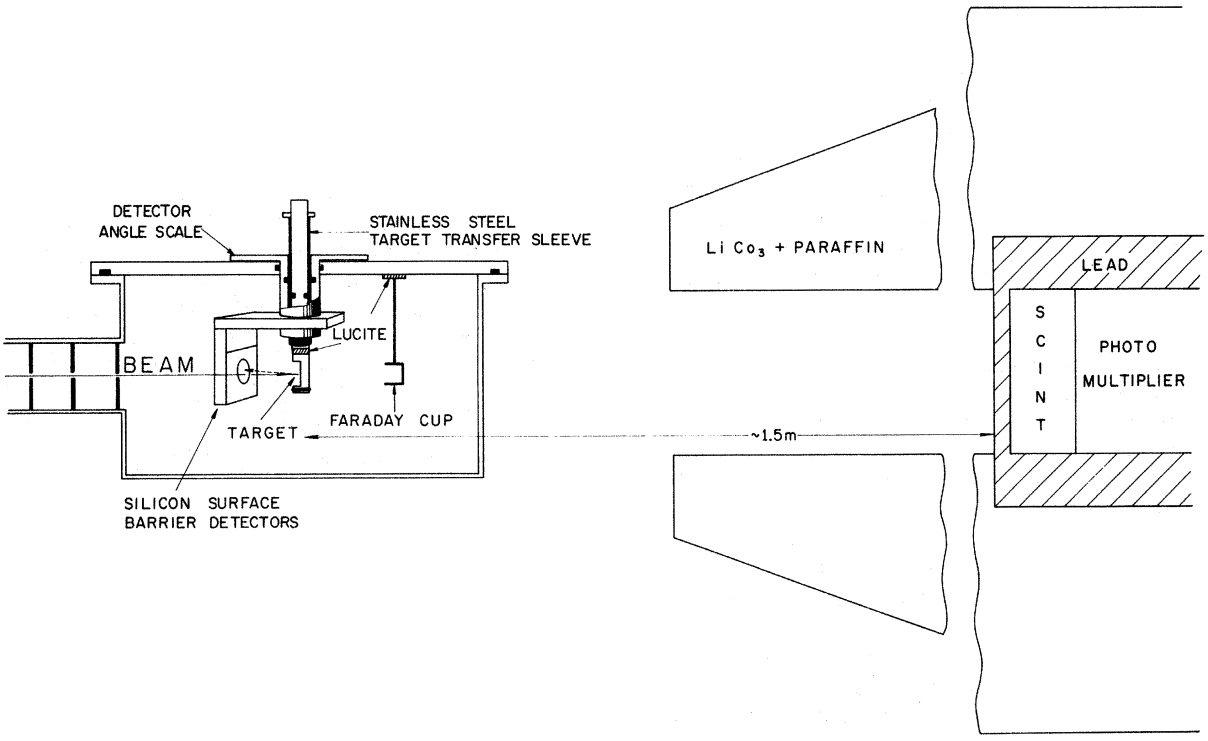

FIG. 1. Experimental apparatus showing target chamber, neutron detector, and $LiCO_3$ collimator used at CIT.

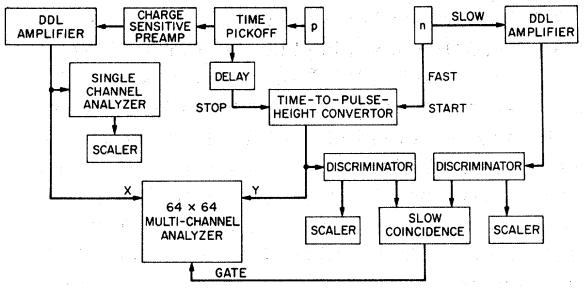

FIG. 2. Schematic diagram of the electronics used in the coincidence measurements.

The "kinematic curves" corresponding to the ^{11}B-(^{3}He, np) reaction leaving ^{12}C in its ground state and first two excited states are very prominent. In addition there is a strongly populated line arising from the ^{11}B(^{3}He, $p\gamma$) and ^{11}B(^{3}He, $d\gamma$) reactions which are also recorded because of the finite efficiency for γ detection in the plastic scintillator. As the γ rays all have the same time of flight, the curve of this line may be used to correct for the variation with proton energy of the trigger time in the proton-detector time-pickoff unit. The enhancements on the kinematic curves at coordinates $[E_n, E_p$ (MeV)] of (1.1, 11.2) and (1.1, 7.0) correspond to decay of the ^{13}N (15.07 MeV, $T=\frac{3}{2}$) level to the ground state and 4.44-MeV state of ^{12}C.

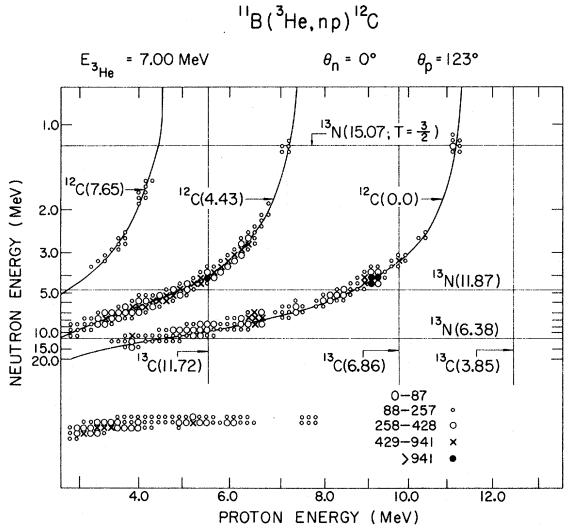

FIG. 3. Two-dimensional spectrum from the reaction ^{11}B(^{3}He,np)^{12}C with proton energy as the abscissa and neutron time of flight as the ordinate. Solid curves are kinematic curves corresponding to levels of ^{12}C. Horizontal (vertical) straight lines indicate the calculated positions of excited states of ^{13}N(^{13}C) from the ^{11}B(^{3}He,n) [^{11}B(^{3}He, p)] reaction. Events forming a curve in the lower left corner of the spectrum are due to particle γ-ray coincidences. Background due to random coincidences has been subtracted.

As may be seen in Fig. 3 the (1.1, 11.2) enhancement lies between the proton energies corresponding to the 3.85- and 6.86-MeV levels of ^{13}C and therefore could not correspond to the decay of any known level of ^{13}C. However the level density in ^{13}C is sufficiently high near the (1.1, 7.0) enhancement that a sequential process through ^{13}N (15.07) cannot be assumed without further checks.

This latter enhancement is clearly observed at proton-detector laboratory angles of 90, 123, and 140°. At all angles the observed neutron energy corresponded to the 15.07-MeV level of ^{13}N, whereas the proton energies would have corresponded to excitation energies of 10.0, 9.85, and 9.75 MeV in ^{13}C. This enhancement was therefore attributed to the proton decay of the 15.07-MeV level of ^{13}N.

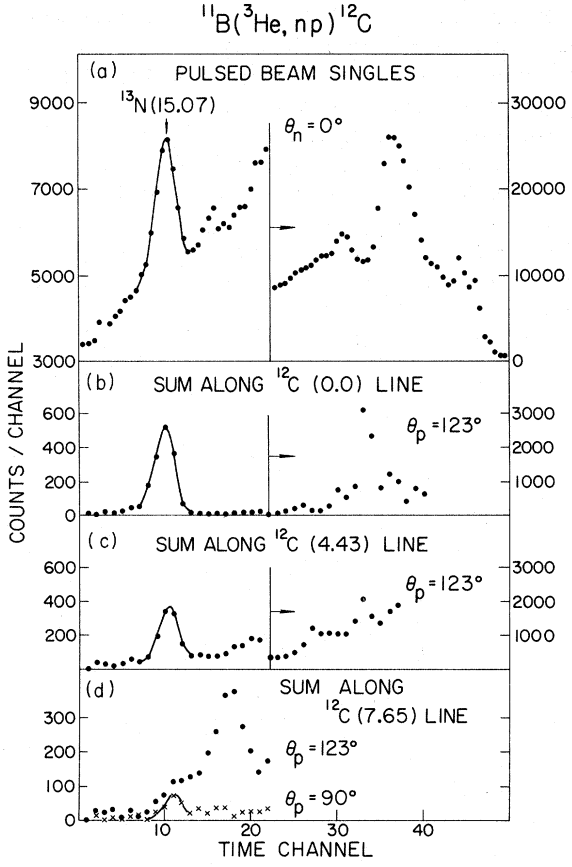

FIG. 4. (a) Neutron time-of-flight spectrum of the ^{11}B(^{3}He,n) reaction at $E_{^3He}$ = 7.00 MeV obtained with the CIT pulsed-beam facility with a flight path of 1.5 m. (b)–(d) Projections of the spectrum of Fig. 3 onto the neutron time-of-flight axis, obtained by summing over four proton-energy channels centered on the kinematic curves corresponding to the ground state and first two excited states of ^{12}C. The number of counts in the peaks corresponding to the 15.07-MeV $T=\frac{3}{2}$ level, relative to the peak observed in spectrum (a) was used to determine the the branching ratios to the energy levels of ^{12}C.

Similar methods were used throughout this work to determine the sequential nature of observed enhancements.

The background from random coincidences has been subtracted from the spectrum shown in Fig. 3. These coincidences are essentially uniform along the time axis, but reflect the variation of count rate with charged-particle energy on the proton-energy axis. The average number of random coincidences in each proton-energy channel was determined by summing counts in the region of the spectrum between the particle-γ coincidence curve and the kinematic curve corresponding to the ground state of ^{12}C. This region contains no true coincidences from the (^{3}He, np) reaction on ^{11}B or any likely target contaminants.

Data analysis was facilitated by the use of a computer program which projected the kinematic curves on either the time or the energy axis. The projection on the time axis was made by summing, for each time channel, a given number of energy channels centered around one of the kinematic curves. Each such projection represents a time spectrum of neutrons in coincidence with protons leaving ^{12}C in one of its various states. In Fig. 4(b)–(d) we display projected spectra of n-p coincidences leaving ^{12}C in its ground state and first two excited states. These may be compared with Fig. 4(a) which is a singles pulsed-beam neutron time-of-flight spectrum for the ^{11}B(^{3}He, n)^{13}N reaction obtained under identical conditions. A peak is observed at channel 11 (67 nsec/m) in all four spectra which corresponds to the lowest $T=\frac{3}{2}$ level of ^{13}N as discussed above. The ratios of the peak areas in the three projected spectra to the appropriately normalized peak area of the singles spectra may be used to determine the absolute branching ratios for decay to the various states of ^{12}C.

The formula used to evaluate the differential

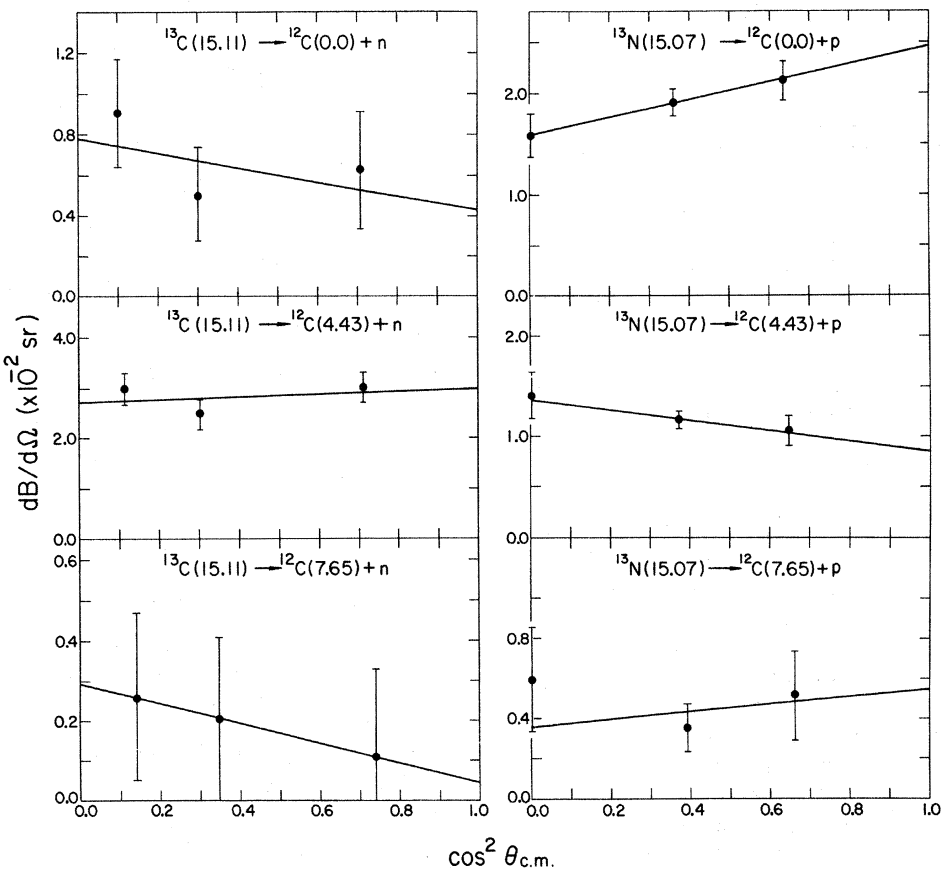

FIG. 5. Differential branching ratios for decays of the 15.1-MeV $T=\frac{3}{2}$ levels of ^{13}C and ^{13}N to the ground state and first two excited states of ^{12}C. Solid lines are least-sqaures fits to the data of the formula $dB/d\Omega = A_0 + A_2 P_2(\cos\theta)$. The fit for ^{13}N(15.07) → ^{12}C(7.65) + n has been constrained to have the same ratio of A_2/A_0 as that determined for ^{13}N(15.07) → ^{12}C(0.0) + n (see Appendix). Branching ratios are defined as $4\pi A_0$.

branching ratios in the center-of-mass system of the recoiling ^{13}N nuclei was

$$\frac{dB(\theta_p)}{d\Omega_{\text{c.m.}}} = \frac{N_0(\text{coinc})}{N_{\text{mon}}(\text{coinc})} \frac{N_{\text{mon}}(\text{sing})}{N_0(\text{sing})} \frac{d\Omega_{\text{lab}}}{d\Omega_{\text{c.m.}}} \frac{1}{\Delta\Omega_{\text{lab}}},$$

where N_0(sing) and N_0(coinc) are the number of counts in the peak corresponding to the ^{13}N ($T=\frac{3}{2}$) level in the singles spectrum and in the projection of the kinematic line from the coincidence spectrum. These numbers were corrected for the dead times of the multichannel analyzers. N_{mon}(sing) and N_{mon}(coinc) are the number of counts obtained in the peak from the ^{11}B(^{3}He, p)^{13}C(0.0) reaction during the accumulation of the singles and coincidence spectra. $\Delta\Omega_{\text{lab}}$ is the solid angle of the proton detector in steradians.

Differential branching ratios were determined at three different angles and are shown in Fig. 5. Since the 15.07-MeV $T=\frac{3}{2}$ state of ^{13}N has spin $\frac{3}{2}$, we must have

$$dB/d\Omega(\theta_{\text{c.m.}}) = A_0 + A_2 P_2(\cos\theta_{\text{c.m.}}) = A_0 + A_2(3\cos^2\theta - 1)/2 \quad (1)$$

(see Appendix). The data appear to be well described by a straight line when plotted versus $\cos^2\theta$ and the solid lines in Fig. 5 are least-squares fits of formula (1) to the data. The absolute branching ratios [BR(%) $= 4\pi A_0$] obtained from these fits are listed in Table I. Branching ratios are presented for nucleon decay to the ground state BR(0_1^+) and first two excited states of ^{12}C-[BR(2_1^+), BR(0_2^+)].

The errors in the branching ratios are dominated by the statistical uncertainties of the peak area in the coincidence spectra and the uncertainty in the subtraction of the background under the peak in the singles spectra. Because of the poor energy resolution of both the neutron and proton detectors employed in the coincidence apparatus, we had to consider the possibility that unresolved nearby peaks could not be distinguished from those due to the 15.07-MeV state of ^{13}N, and that we were, in fact, measuring the combined branching ratios of more than one state. Such peaks could arise from contaminants in the ^{11}B target or from levels in ^{13}N that lie close to the lowest $T=\frac{3}{2}$ level and might be appreciably populated in the (^{3}He, n) reaction. We do not expect any levels in ^{13}N to affect our results significantly, as higher resolution studies of the ^{11}B(^{3}He, n) reaction at 7.0 MeV (see Ref. 29 and Fig. 6) have shown that the peak ascribed to the lowest $T=\frac{3}{2}$ level of ^{13}N corresponds to a level with a natural width less than 15 keV. Any interfering level would therefore have to be narrow and lie within 15 keV of the $T=\frac{3}{2}$ level. However, the highly selective ^{11}B(^{3}He, n) reaction shows no peak other than the $T=\frac{3}{2}$ level in the excitation region between 14.7 and 16.9 MeV. In the latest compilation[32] of energy levels of ^{13}N the closest known state lies 300 keV from the 15.07-MeV level.

On the other hand, there is a peak due to the ^{16}O(^{3}He, n)^{18}Ne (1.89-MeV) reaction from oxygen contaminants in the target which falls very close to the $T=\frac{3}{2}$ level in the singles spectra. As proton decay of the ^{18}Ne (1.89-MeV) level is energetically forbidden, there is no contribution from this contaminant in the n-p coincidence spectra. To remove the contribution from the ^{18}Ne(1.89) level in the singles spectra, an additional spectrum was taken under identical conditions, using a WO_3 target. The peaks from ^{18}Ne(0.0) in this spectrum and in the spectrum taken with the ^{11}B target were used to determine the relative amounts of ^{16}O in the two targets. The normalized ^{18}Ne(1.89) peak from the WO_3 target was then subtracted channel

TABLE I. Decay properties of the lowest $T=\frac{3}{2}$ levels in ^{13}C and ^{13}N (Ref. a).

	^{13}C	^{13}N
BR(0_1^+)	0.070 ± 0.018	0.236 ± 0.012
BR(2_1^+)	0.261 ± 0.030	0.150 ± 0.010
BR(0_2^+)	0.026 ± 0.018	0.053 ± 0.015
BR(α_0)	0.019 ± 0.005 [b]	0.049 ± 0.027
BR(α_1)	...	0.039 ± 0.039
BR(α_2)	...	0.072 ± 0.045
$\theta^2(0_1^+)/\theta^2(2_1^+)$ [c]	0.173 ± 0.026	1.13 ± 0.07
Γ_{TOTAL}	6.7 ± 1.7 keV [d]	0.82 ± 0.20 keV [e]
	4.3 ± 0.7 keV [f]	1.03 keV [g]
$\Gamma_{\text{TOTAL}}^{(\text{adopted})}$	5.0 ± 0.7 keV	0.82 ± 0.20 keV
$\Gamma_{0_1^+}$	0.35 ± 0.10 keV	0.19 ± 0.05 keV
$\Gamma_{2_1^+}$	1.31 ± 0.24 keV	0.12 ± 0.03 keV
$\Gamma_{0_2^+}$	0.130 ± 0.092 keV	0.043 ± 0.016 keV
Γ_{α_0}	0.095 ± 0.028 keV	0.040 ± 0.024 keV
Γ_{α_1}	...	0.032 ± 0.032 keV
Γ_{α_2}	...	0.059 ± 0.040 keV
$\Gamma_{\gamma_{0_{M1}}}$	23.3 ± 2.6 eV	23.3 ± 3.6 eV
Γ_{γ_0}	22.7 ± 2.6 eV	23.0 ± 3.6 eV
	(0.325 W.u.)	(0.318 W.u.)
Γ_{γ_1}	...	<3.3 eV

[a] The branching ratios are from this work except for Γ_{α_0} for ^{13}C which is taken from Ref. 60. Other quantities are obtained as described in Sec. 5A.

[b] P. H. Nettles and D. C. Hensley, Bull. Am. Phys. Soc. 14, 1168 (1969).

[c] The error in the ratio of reduced widths is smaller than implied by the uncertainties in the branching ratios because of systematic effects which cancel in the ratio of reduced widths. Penetration factors were evaluated at a radius of 4.0 fm.

[d] Reference 34.

[e] References 20, 28, and present work.

[f] References 21 and 28.

[g] Reference 27.

by channel from the spectrum of the ^{11}B target. The shapes of the backgrounds under the ^{18}Ne(0.0) and the ^{13}N ($T=\frac{3}{2}$) peaks in the spectrum from the ^{11}B target were determined from higher resolution spectra taken at flight paths up to 3.3 m (see Fig. 6). However, the uncertainty in the shape of this background remained the major source of error in our result for the branching ratio to the ground state of ^{12}C. To evaluate the accuracy with which this background subtraction was performed, the peak shape obtained in the singles run [after subtraction of the ^{18}Ne(1.89) peak and the background] was compared with the peak shape from the coincidence spectrum, projected on the time axis. Figure 7 illustrates the similarity of the shapes.

The error in the branching ratio to the ground state of ^{12}C was determined as the quadratic sum of the following contributions: uncertainty in the background subtraction under the $T=\frac{3}{2}$ peak in singles spectrum (4.8%); uncertainty in subtraction of the contribution to singles spectrum from ^{18}Ne (1.89 MeV) (2.2%); statistical error on peak in coincidence spectrum (2.8%); uncertainty in solid angle of proton detector (1%). All other sources of error are believed to be negligible. It should be noted that the uncertainties in the singles spectra do not contribute to the errors in the determination of the relative branching ratios to various states of ^{12}C, so that the ratios of branching ratios are inherently more accurate than the absolute branching ratios.

Since the angular correlation of the p decays to ^{12}C(0.0) is very anisotropic, we can infer that the ^{13}N substates are unequally populated, indicating that processes other than $L=0$ stripping are involved in the reaction mechanism. Since the outgoing neutron has an energy of only 1 MeV this is not surprising. Using the correlation theory given in the Appendix we find that the ratio of the reduced matrix elements for $p_{1/2}$ and $p_{3/2}$ emission is 2.1 ± 2.4.

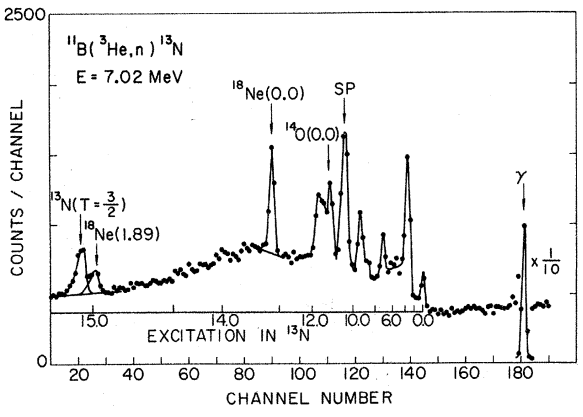

FIG. 6. Pulsed-beam neutron time-of-flight spectrum at a flight path of 3 m from the (^{3}He,n) reaction on a ^{11}B target, showing contributions from oxygen and carbon contamination in the target. The spurious peak (SP) results from γ rays produced by the beam striking collimators a few meters away from the target.

B. Alpha Decays of the 15.07-MeV $T=\frac{3}{2}$ Level of ^{13}N

The apparatus and methods used in this measurement were similar to those described in Sec. 2A. The α detector was a 50-μm-thick surface-barrier detector subtending a solid angle of 12 msr. A single α-n coincidence spectrum was obtained at $E(^3\text{He})=7$ MeV for detector angles $\theta_n=0°$, $\theta_p=51°$. For these conditions $P_2(\cos\theta_{\text{c.m.}})\approx 0$ so that this measurement is sufficient to determine the branching ratios. For this measurement the peak from elastically scattered ^{3}He ions was used as a monitor of beam-target interactions.

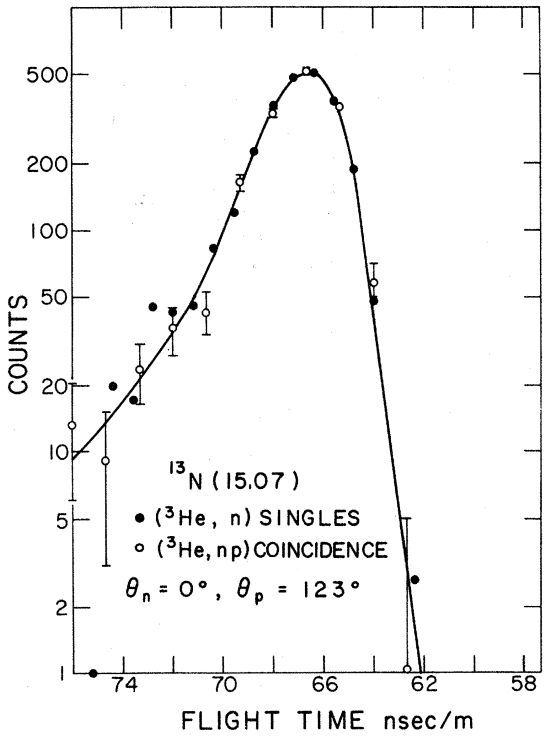

FIG. 7. Comparison of neutron time-of-flight peak shapes obtained for the ^{11}B(^{3}He,n)^{13}N (15.07) reaction in a singles spectrum using a pulsed beam and in a coincidence spectrum in which timing was derived from protons decaying to the ground state of ^{12}C. A linear background has been subtracted in each case and an additional contribution from the ^{16}O(^{3}He,n)^{18}Ne (1.89) reaction on oxygen target contamination has been subtracted from the singles spectrum. The solid curve is included to guide the eye.

The α-n coincidence spectra showed a kinematic curve corresponding to the ground state of ^{9}B and considerable yield in the region of the excited states of ^{9}B. From enhancements on the kinematic curves, branching ratios of $(4.9 \pm 2.7)\%$, $(3.9 \pm 3.9)\%$, and $(7.2 \pm 4.5)\%$ were determined for α decays of the 15.07-MeV, $T = \frac{3}{2}$ level of ^{13}N to the 0.0-, 1.5-, and 2.33-MeV states of ^{9}B, respectively.

An enhancement in yield was also observed at a neutron flight time corresponding to the $T = \frac{3}{2}$ level in ^{13}N, and at charged-particle energies between the 1-MeV lower energy cutoff and 2.5 MeV. This region could correspond to α decays to the ^{5}Li + α continuum and/or proton decays to the 10.84- and 11.83-MeV levels of ^{12}C. For decay to the continuum the angular correlation is no longer simply $A_0 + A_2 P_2(\cos\theta_{\text{c.m.}})$ and so it is impossible to calculate a branching ratio for decay by this mode. However, there is a significant yield observed in this region, which could contribute a large proportion of the remaining decay modes of the ^{13}N($T = \frac{3}{2}$) level. [Note that the sum of the known proton and α-decay modes is only $(60 \pm 14)\%$.]

C. Neutron Decays of the 15.11-MeV $T = \frac{3}{2}$ Level of ^{13}C

The lowest $T = \frac{3}{2}$ level of ^{13}C has an excitation energy of 15.106 ± 0.002 MeV,[33,34] a width of ~5 keV,[34,28] and $J^{\pi} = \frac{3}{2}^{-}$.[33] The apparatus and techniques used to study the isospin-forbidden neutron decays of this state were similar to those described in Sec. 2A. The 15.11-MeV state was populated in the ^{11}B(^{3}He, p) reaction, which preferentially populates this state[33] at 0°, and decay neutrons were detected at a number of laborabory angles. Measurements were performed at incident energies of 7.5 and 6.6 MeV using the CIT EN tandem accelerator, and at 7.5 MeV using the Chalk River MP tandem. Better statistical accuracy was obtained in the last measurement at Chalk River, and the following discussion is restricted entirely to it.

Protons from the ^{11}B(^{3}He, p) reaction were detected in a 1000-μm totally depleted silicon surface-barrier detector at 0°, and neutrons in coincidence with these protons were detected at a distance of 1 m in a 5-cm-thick by 11.3-cm-diam NE102 plastic scintillator coupled to an XP1040 photomultiplier with an ORTEC model 271 constant fraction timing base. Three parameter events, consisting of silicon-detector energy, silicon-detector to photomultiplier time difference, and photomultiplier pulse height were recorded on magnetic tape. A 64×128-channel spectrum of neutron flight time versus proton energy was recorded on line by means of a PDP 1 computer, to monitor the experiment, and playback of the tapes and subsequent data analysis were performed using the Chalk River PDP 10 and CDC 6600 computers.

The protons from the ^{11}B(^{3}He, p) reaction populating the 15.11-MeV state were observed at 0° in order to align the recoiling nuclei and provide a neutron angular distribution of the form $A_0 + A_2 P_2(\cos\theta)$ (see Appendix.) In addition, the proton yield is highest at 0°, so these two features made it necessary to tolerate the poor energy resolution [full width at half maximum (FWHM) ≈ 250 keV] obtained when foils (17 mg/cm^2 of Ni followed by 10 mg/cm^2 of Al) were introduced to stop the incident beam. We are satisfied, however, that our branching ratio measurements are not distorted by unresolved particle groups. Groups arising from (^{3}He, d) reactions on ^{11}B or the target contaminants, and from (^{3}He, p) reactions on target contaminants lie along different curves in the two parameter spectra and cause no difficulty. The only difficulty could arise from levels in ^{13}C. However, high-resolution studies of the ^{11}B(^{3}He, p) reaction at 12-MeV incident energy[33] failed to reveal the presence of any other states in ^{13}C within 500-keV excitation energy of the 15.11-MeV state. In addition, the proton group leading to the $T = \frac{3}{2}$ level was found to have a symmetrical shape with a total observed width of 17.5 keV FWHM, due predominantly to experimental energy resolution. Since no known[32] narrow level ($\Gamma < 100$ keV) of ^{13}C falls within 1.5 MeV of the 15.11-MeV level it is most unlikely that a very narrow $T = \frac{1}{2}$ state is unresolved from the $T = \frac{3}{2}$ state in the high-resolution studies.

The peak due to the $T = \frac{3}{2}$ level was somewhat obscured in the singles spectra from the silicon detector [Fig. 8(a)] by a large peak resulting from the ^{3}He(^{1}H, p)^{3}He reaction on hydrogen contamination in the target and in the foils. However, a peak due to the 9.9-MeV level of ^{13}C was cleanly resolved in the spectra, and was used as a monitor of beam-target interactions. This peak is clearly resolved from any peaks which might result from (^{3}He, p) or (^{3}He, d) reactions on ^{12}C, ^{16}O, or ^{10}B, which are the only likely target contaminants. To determine the population of the $T = \frac{3}{2}$ level relative to the 9.9-MeV level, both levels were observed with high resolution at 0° in the 61-cm double-focusing magnetic spectrometer at CIT where they stood out cleanly above background.

The neutron detector used at Chalk River was contained in a cylindrical lead shield 2.5 cm thick and a lead plate 1.3 cm thick was placed in front of the detector to reduce the background of γ rays from the target. This shield is similar to the lead shield used at CIT, but does not include the large $LiCO_3$ loaded paraffin collimator. Tests at CIT[35]

showed that the presence of this collimator affected neutron efficiencies by less than 15% and so the efficiency of the neutron detector was taken to be the same as that of the CIT detector, with an additional error in absolute efficiency of ±15%. The efficiency curve for the CIT detector is shown in Fig. 9. The experimental points were determined using the known cross sections for the $D(d,n)^{36}$ and $T(p,n)^{37}$ reactions. For neutron energies between 1.95 and 10.75 MeV the efficiency was measured using the $D(d,n)$ reaction and a gas-target cell to obtain absolute efficiencies. Relative efficiencies for neutrons with energies less than 2.6 MeV were found using the $T(p,n)$ reaction and were matched onto the absolute efficiencies from the $D(d,n)$ reaction. The solid curve in Fig. 9 is calculated from the $H(n,n)$ scattering cross section for a recoil-proton cutoff energy of 450 keV. The dashed line is an approximation to the data used for interpolation of the efficiencies used in the present work. The uncertainty in the relative efficiency is estimated to be less than ±5% and the uncertainty in absolute detection efficiency is estimated to be ±10% for the CIT detector and ±18% for the Chalk River detector. The pulse-height threshold for the neutron detector was set to be $\frac{1}{8}$ of the midpoint of the Compton edge observed with a ^{137}Cs source and was checked frequently to maintain constant neutron-detection efficiency.

Neutron-proton coincidence spectra were obtained for neutron-detector laboratory angles of 105, 123, and 145° at a detector distance of 1 m. Enhancements were observed in all cases at points corresponding to decay of the ^{13}C(15.11-MeV) level to the ground state and 4.43-MeV level of ^{12}C. Figure 8 shows projections on the proton-energy axis of the kinematic curves corresponding to the lowest three states of ^{12}C, as well as the singles spectrum obtained in the proton detector. The peaks corresponding to decays to the ground state

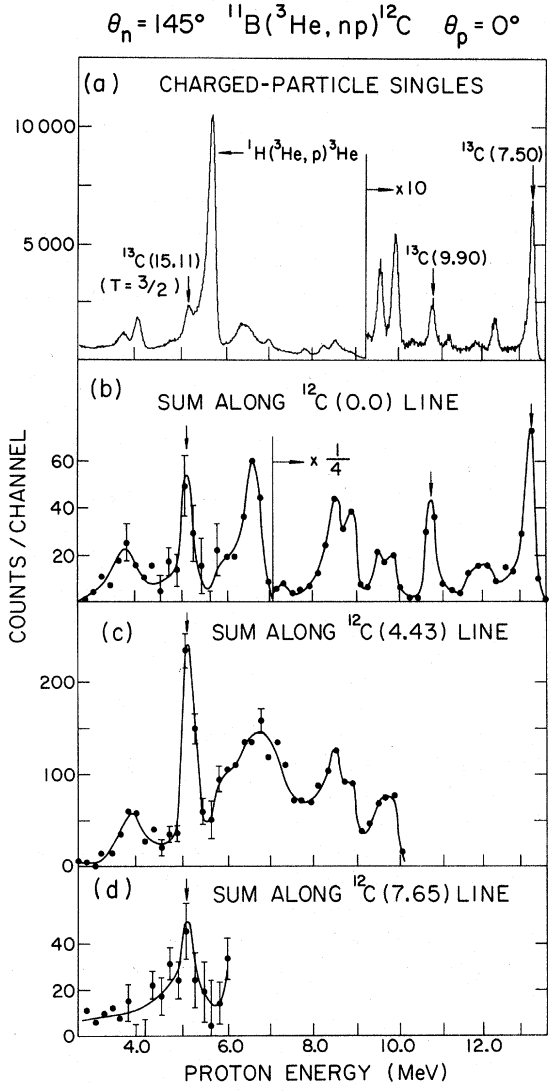

FIG. 8. (a) Charged-particle singles spectrum obtained at 0° with a 7.5-MeV ^3He beam incident on a 75-$\mu g/cm^2$ ^{11}B self-supporting target, followed by a 17-mg/cm^2 Ni foil and a 10-mg/cm^2 Al foil. The large peak at 5.5 MeV is due to hydrogen contamination in the target and foils. (b)–(d) Projections onto the proton-energy axis of the kinematic curves corresponding to the ground state and first two excited states of ^{12}C, observed in the $^{11}B(^3He,np)^{12}C$ reaction with similar target conditions to Fig. 8(a).

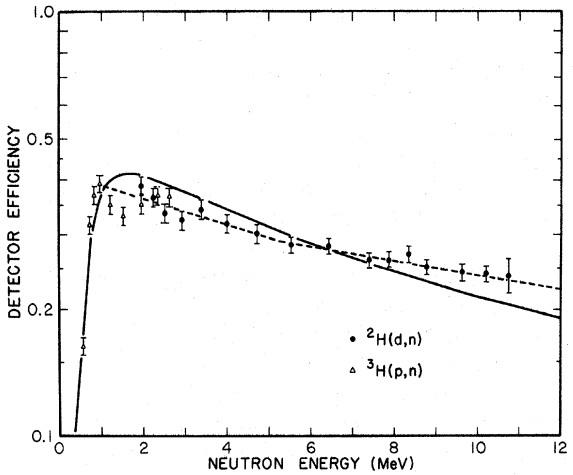

FIG. 9. Neutron detection efficiency, determined from the $D(d,n)$ reaction (closed circles) and the $T(p,n)$ reaction (open circles). The solid curve is calculated from the $H(n,n)$ scattering cross section, for a recoil-proton cutoff energy of 440 keV. The dashed lines are approximations to the data, used to determine efficiency values for all calculations in the present work.

and 4.43-MeV level of ^{12}C are clearly observed, but the decay branch to the 7.65-MeV level of ^{12}C is much weaker.

Differential branching ratios as a function of angle were calculated from the following expression

$$\frac{dB}{d\Omega_{\text{c.m.}}} = \frac{N_n(\text{coinc})}{N_{9.9}(\text{sing})} \frac{N_{9.9}(\text{mag})}{N_{15.11}(\text{mag})} \frac{d\Omega_{\text{lab}}}{d\Omega_{\text{c.m.}}} \frac{1}{\Delta\Omega_n} \frac{1}{\epsilon_n},$$

where N_n(coinc) is the number of counts in the peak corresponding to the ^{13}C 15.11-MeV level in the projection of the kinematic curve from the coincidence spectrum. $N_{9.9}$(sing) is the number of counts in the peak due to the ^{11}B(^{3}He, p)^{13}C(9.9-MeV) reaction in the singles spectrum. $N_{9.9}$(mag) and $N_{15.11}$(mag) are the yield in the peaks corresponding to ^{13}C (9.9 MeV) and (15.11 MeV) in the high-resolution spectra obtained with the CIT magnetic spectrometer. All of these numbers have been corrected for the dead times of the related electronic circuitry. ϵ_n is the efficiency of the neutron detector as determined from the dashed curve in Fig. 9 and $\Delta\Omega_n$ is the solid angle of the neutron detector, in steradians.

The values obtained for $dB/d\Omega$ are plotted in Fig. 5. The main errors in the measurement, other than statistical errors in N_n(coinc) were 10% from the N(mag) ratio and 18% from the neutron-detection efficiency. Branching ratios were determined by least-squares fits to the data as shown by solid lines in Fig. 5. Results obtained at two energies at CIT agreed within the errors with the result obtained at Chalk River and a weighted average of the results is listed in Table I. As the relative neutron-detection efficiencies are better known than the absolute values, the ratios of branching ratios are more accurately determined than is indicated by the individual numbers.

The determination of the slope of the angular correlation for the decays to ^{12}C(0.0) is difficult due to the small branching ratios for this branch. Within the poor statistical accuracy available, the correlation appears to be close to isotropic. This is to be expected if the reaction proceeds by $L=0$ stripping. Presumably the fact that the outgoing proton in the ^{11}B(^{3}He, p)^{13}C is considerably more energetic than the neutron in the ^{11}B(^{3}He, n)^{13}N reaction accounts for the difference in the two cases. As a consequence of this isotropy, we were unable to separate the $j=\frac{1}{2}$ and $j=\frac{3}{2}$ contributions to the decays to the 2^+ state of ^{12}C.

Using techniques similar to those described above, branching ratios were also measured for the 9.9- and 11.7-MeV $T=\frac{1}{2}$, $J^\pi=\frac{3}{2}^-$ levels. The population of these levels in the ^{11}B(^{3}He, p)^{13}C reaction was determined using an annular particle telescope (200-μm ΔE and 1000-μm E detector) at 0°, and the branching ratios were determined by observing coincidences between the E detector and the neutron detector. The particle telescope permitted both these levels to be clearly resolved from other levels populated in the (^{3}He, p), (^{3}He, d), and (^{3}He, t) reactions. The observed branching ratios are listed in Table III. These levels are of particular interest since they have $J^\pi=\frac{3}{2}^-$ and may therefore be mixed into the $T=\frac{3}{2}$ level.

3. BRANCHING-RATIO MEASUREMENTS FOR MASS 17

A. Proton Decays of the Lowest $T=\frac{3}{2}$ Level of ^{17}F

The lowest $T=\frac{3}{2}$ level of ^{17}F has an excitation energy of 11.197 ± 0.004 MeV,[26] a width of approximately 0.5 keV,[38,39] and $J^\pi=\frac{1}{2}^-$.[29,38] We have studied the isospin-forbidden proton decays of this level to the ground and unresolved first and second excited states of ^{16}O using a technique similar to that employed in the ^{13}N measurement. The state was populated in the ^{15}N(^{3}He, n) reaction which preferentially populates the 11.197-MeV state.[29]

Measurements were performed at CIT, using a cylindrical brass scattering chamber having a diam of 8.1 cm and a wall thickness of 0.32 mm. Highly enriched ^{15}N gas was contained in a thin gas cell designed so that the proton and neutron detectors both viewed the total volume of interaction between the incident beam and the target gas. The beam entered the cell through a 10^{-3}-mm-thick circular nickel foil and was stopped in a tantalum disk which formed the rear wall of the cell. A 0.057-mm-thick aluminum foil was placed immediately in front of the counter to stop ^{3}He ions elastically scattered from the nickel foils and beam stop. A 1000-μm surface-barrier counter was used to detect the charged particles. The counter subtended a solid angle which was typically 17 msr. The neutron detector was the same one used at CIT to study the ^{13}C decays. Since the 11.20-MeV state of ^{17}F has spin $\frac{1}{2}$, its decays are isotropic in its rest frame and, in principle, a measurement at one beam energy and one decay angle suffices to determine the branching ratio. However, measurements were made at several different combinations of beam energy and decay angle in order to ensure that the enhancements we were ascribing to decays of the 11.20-MeV $T=\frac{3}{2}$ state were in fact due to proton decays of a state in ^{17}F and not to neutron decays of states in ^{17}O. In order to obtain the relative normalization of the coincidence and pulsed-beam singles spectra, the energy spectrum from the surface-barrier

counter was simultaneously recorded in a separate 200-channel analyzer. The number of counts in the isolated peak from the ^{15}N(^{3}He, d_0) reaction served as an accurate monitor independent of beam-position fluctuations and gas-pressure changes.

The branching ratio for proton decays to the ground state of ^{16}O was determined from five separate coincidence spectra taken at incident energies of 8.25 and 8.44 MeV and decay angles of 90, 110, 120, and 135°. The energies and angles were chosen to place the enhancement from the decays of the ^{17}F ($T=\frac{3}{2}$) level between the strong enhancements due to levels in ^{17}O at 4.55 and 5.08 MeV. The neutron detector was placed at zero degrees and 1.5 m from the target. Sample singles and coincidence spectra are shown in Fig. 10. The proton decays of the lowest $T=\frac{3}{2}$ level of ^{17}F to the ground state of ^{16}O are seen as a weak enhancement located between intense groups from neutron decays of ^{17}O.

In our measurements of the decay of the ^{17}F $T=\frac{3}{2}$ level to the unresolved 6.06- and 6.13-MeV states of ^{16}O, the density of ^{17}O states which produced enhancements in the same region was so high that it was not possible to resolve the $T=\frac{3}{2}$ decays from them. However, we found that the levels were so dense as to produce a rather uniform background upon which the ^{17}F enhancement appears. This is illustrated in Fig. 11 which shows the projection on the neutron axis of the kinematic curve corresponding to the 6.05- and 6.13-MeV levels of ^{16}O. Parts a, b, and c correspond to ^{3}He incident energies of 9.18, 9.03, and 8.93 MeV, respectively. Enhancements due to the neutron decay of levels in ^{17}O are expected to occur at a constant neutron flight time, determined by the energy available for the ^{17}O decay and the ^{17}O center-of-mass energy, which is not strongly dependent on the beam energy. On the other hand, enhancements due to the proton decay of the ^{17}F

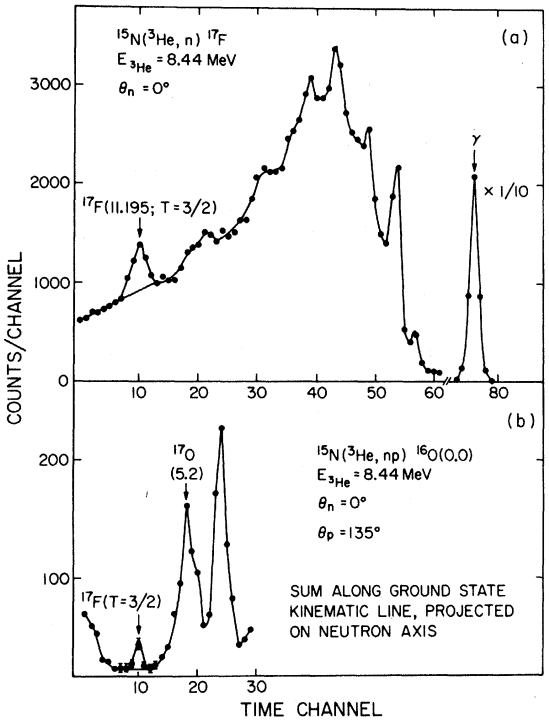

FIG. 10. (a) Neutron time-of-flight spectrum from the ^{15}N(^{3}He,n)^{17}F reaction at $E_{^3He}$ = 8.44 MeV. The peak near channel 76 is due to prompt γ rays. (b) Projection onto the neutron time-of-flight axis of the kinematic curve corresponding to the ground state of ^{16}O, observed in the ^{15}N(^{3}He,np)^{16}O reaction.

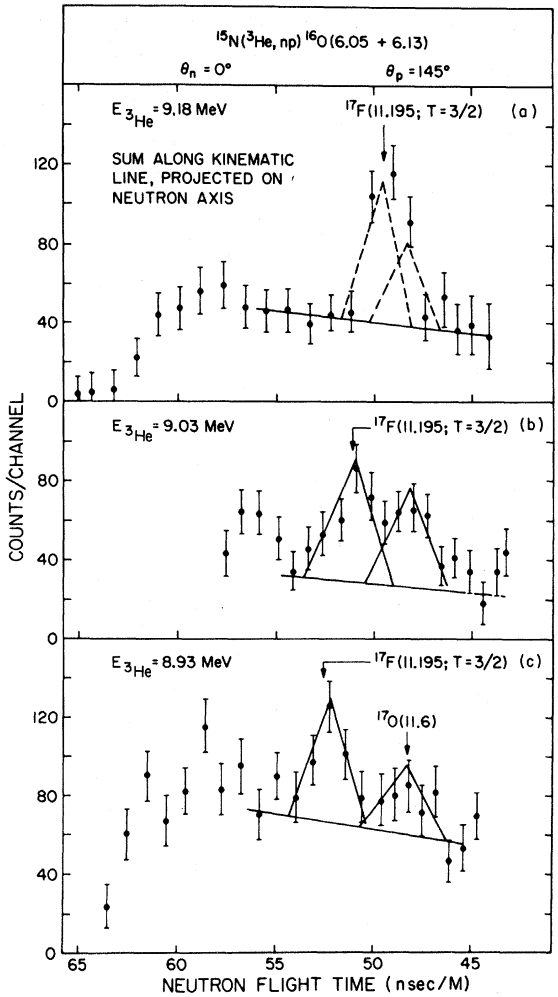

FIG. 11. Projections of the neutron time-of-flight axis of the kinematic curve corresponding to the ^{15}N(^{3}He,np)-^{16}O (6.05 + 6.13) reaction at (a) 9.18-MeV (b) 9.03-MeV and (c) 8.93-MeV incident energy for θ_n = 0°, θ_p = 145°. For a discussion of the peaks see Sec. 3A.

($T=\frac{3}{2}$) level occur at a neutron flight time appropriate to the ^{15}N(^{3}He, n)^{17}F (11.195) reaction, and have different flight times at the three different incident energies. Two peaks may be observed in the spectra, one of which remains fixed at a position corresponding to a level in ^{17}O at 11.6 MeV. The other has a centroid which occurs at the expected position of the ^{17}F ($T=\frac{3}{2}$) level as determined from pulsed-beam, single-counting spectra at the three energies and is assumed to be an enhancement due to the proton decay of the ^{17}F ($T=\frac{3}{2}$) level.

Our branching ratios for the proton decays of the lowest $T=\frac{3}{2}$ level of ^{17}F are listed in Table II. The quoted errors include contributions from counting statistics, uncertainty in the background subtractions, dead-time corrections, and the solid angle subtended by the counter. Our branching ratios are in good agreement with those obtained completely independently[8] from delayed proton emission following the superallowed Fermi β^+ decay of ^{17}Ne, also listed in Table II. In the delayed proton work it was possible to resolve the 6-MeV doublet of ^{16}O. The decays were found to proceed predominantly to the 6.13-MeV 3^- state.

B. Neutron Decays of the Lowest $T=\frac{3}{2}$ Level of ^{17}O

The lowest $T=\frac{3}{2}$ level of ^{17}O has been observed in both the ^{15}N(^{3}He, p) and ^{18}O(^{3}He, α) reactions.[40,41] It has an excitation energy of 11.075 ± 0.006 MeV, a width $\Gamma=5\pm1$ keV,[42] and $J^\pi=\frac{1}{2}^-$.[40,41] In our first attempt to measure branching ratios for neutron decays of the 11.08-MeV $T=\frac{3}{2}$ state we populated it by the ^{15}N(^{3}He, p) reaction. The beam entered a gas cell with a diameter of 1.2 cm through a 10^{-3}-mm-thick nickel foil and protons left the cell at 0° through a 5×10^{-2}-mm-thick copper foil which was sufficient to stop the ^{3}He ions. Otherwise the apparatus was identical to that employed for the ^{17}F decays. Since the resolution of the silicon detector for protons populating the $T=\frac{3}{2}$ level of ^{17}O was degraded by the foil to 250 keV FWHM, the population of the $T=\frac{3}{2}$ level could not be determined accurately from the silicon-detector spectra. Therefore the 61-cm magnetic spectrometer at CIT was used to determine the population of the $T=\frac{3}{2}$ level relative to the 7.12-MeV state of ^{16}O formed in the ^{15}N(^{3}He, d) reaction. The latter group was the most prominent peak in the silicon-

TABLE II. Decay properties of the lowest $T=\frac{3}{2}$ levels of ^{17}O and ^{17}F (Ref. a).

	^{17}O	^{17}F	
		Present work	Ref. 8
BR(0_1^+)	0.91 ± 0.15	0.088 ± 0.016	0.10 ± 0.02
BR(0_2^+)	0.05 ± 0.02 [b]	0.23 ± 0.05 [b]	<0.03
BR(3_1^-)			0.22 ± 0.02
BR(2_1^+)	...		0.24 ± 0.06
BR(1_1^-)	...		0.44 ± 0.04
BR(α_0)	0.06 [c]		<0.07
$\theta^2(0_1^+)/\theta^2(3_1^+)$ [d]	0.31 ± 0.14	0.065 ± 0.019	
Γ_{TOTAL}	5 ± 1 keV [c]	$0.43^{+0.13}_{-0.22}$ keV [e]	
$\Gamma_{0_1}^+$	4.5 ± 1.2 keV	40^{+10}_{-20} eV	
$\Gamma_{0_2}^+$		<17 eV	
$\Gamma_{3_1}^-$	0.25 ± 0.11 keV	95^{+30}_{-50} eV	
$\Gamma_{2_1}^+$	...	100^{+40}_{-60} eV	
$\Gamma_{1_1}^-$	...	190^{+60}_{-100} eV	
Γ_{α_0}	0.3 keV	<40 eV	
Γ_{γ_1}	...	~4 eV [f]	

[a] Branching ratios are from this work and Ref. 8. Other quantities are obtained as described in Sec. 5B.
[b] Sum of branching ratios to 0_2^+ and 3_1^-.
[c] Reference 42.
[d] The penetration factors are evaluated at a radius of 4.4 fm.
[e] References 38 and 39.
[f] M. Haraken, K. A. Snover, and P. Paul, Bull. Am. Phys. Soc. 17, 98 (1972).

detector spectra and its population was easily determined. In the course of these measurements we discovered that a level of ^{17}O with $T=\frac{1}{2}$, at an excitation energy of 11.023 MeV, which has been observed in the ^{13}C$(\alpha, n\gamma)$ reaction,[43] was also populated significantly in the ^{15}N$(^3$He$, p)$ reaction. In Fig. 12(a) we display a singles-momentum spectrum of protons from the ^{15}N$(^3$He$, p)$ reaction, measured in the magnetic spectrometer, which shows the 11.075- and 11.023-MeV states. Since the 11.075-MeV $T=\frac{3}{2}$ state could not be resolved from the nearby $T=\frac{1}{2}$ level using the coincidence apparatus, we were unable to obtain accurate branching ratios by using the ^{15}N$(^3$He$, p)$ reaction to populate the $T=\frac{3}{2}$ level. We could, however, place limits on the neutron branching ratios of the $T=\frac{3}{2}$ level from our measurements. In a series of ^{15}N-$(^3$He$, np)$ coincidence spectra taken at various incident energies, a strong enhancement at the position expected for decays of the unresolved 11.023- and 11.079-MeV levels of ^{17}O to the ground state of ^{16}O was observed (see Fig. 13). When the enhancement along the kinematic lines corresponding to decays to the first and second excited states of ^{16}O were examined, a peak was found corresponding to decays of the 11.02-MeV state to the 6.13-MeV state of ^{16}O. From such spectra upper limits of 10% and 15% were set for decays of the $T=\frac{3}{2}$ level to the 6.06- and 6.13-MeV states of ^{16}O, respectively. From a knowledge of the relative populations of the 11.079- and 11.023-MeV states a lower limit of 48% was placed on the branching ratio of the $T=\frac{3}{2}$ state to the ground state of ^{16}O.

To obtain more accurate branching ratios for the neutron decays of the lowest $T=\frac{3}{2}$ level of ^{17}O the state was populated in the ^{18}O$(^3$He$, \alpha)$ reaction which populates the 11.079-MeV $T=\frac{3}{2}$ level very strongly and does not populate any nearby $T=\frac{1}{2}$ states. In Fig. 12(b) we display a singles-momentum spectrum of α particles, taken with the 61-cm magnetic spectrometer, set at 10°, which demonstrates the great selectivity of the $(^3$He, $\alpha)$ reaction. Our ^{18}O targets were prepared by oxidizing 10^{-4}-mm-thick nickel foils in an $^{18}O_2$ at-

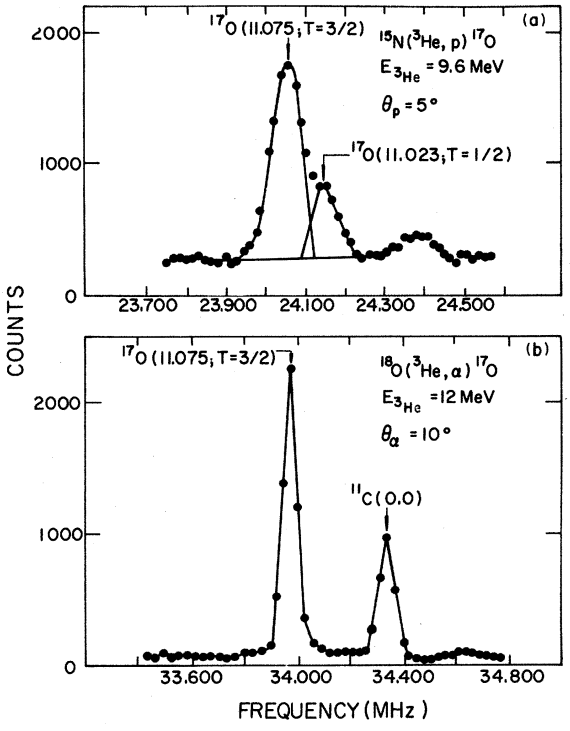

FIG. 12. (a) Spectrum of protons detected in the CIT 81-cm radius magnetic spectrometer from the ^{15}N-$(^3$He$, p)^{17}$O reaction at an incident energy of 9.6 MeV. The ordinate is NMR frequency, proportional to particle momentum. (b) Spectrum of α particles from the ^{18}O-$(^3$He$, \alpha)^{17}$O reaction at 12-MeV incident energy. The peak labeled ^{11}C(0.0) is due to the ^{12}C$(^3$He$, \alpha)$ reaction on carbon contamination in the target.

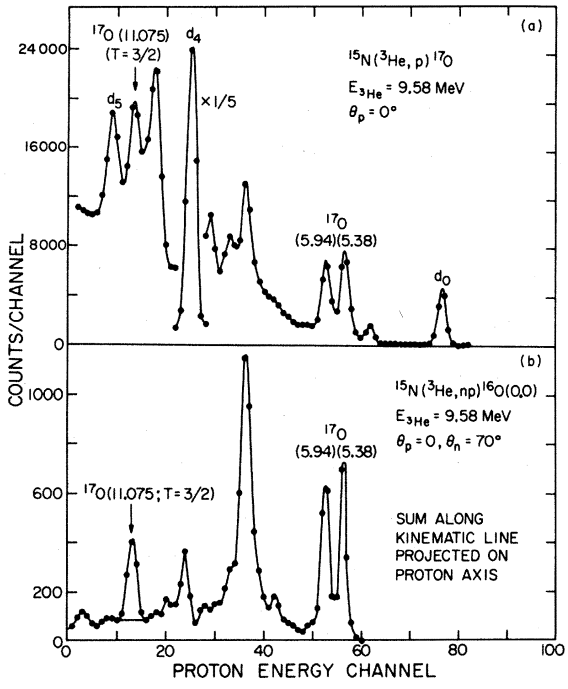

FIG. 13. (a) Energy spectrum of protons and deuterons from the ^{15}N$(^3$He$, p)^{17}$O and ^{15}N$(^3$He$, d)^{16}$O reactions at 9.58-MeV incident energy. Clearly visible are the peaks corresponding to the ^{17}O (11.075; $T=\frac{3}{2}$) level and the d_0 peak which was monitored during all ^{15}N$(^3$He$, np)^{16}$O coincidence runs. (b) Projection on the proton axis of the kinematic line due to the ^{15}N$(^3$He$, np)^{16}$O (0.0) reaction at an incident energy of 9.58 MeV, for $\theta_p=0°$, $\theta_n=70°$. The peak near channel 12 is assumed to correspond to decays of the ^{17}O (11.075) level to the ground state of ^{16}O.

mosphere. Due to the Coulomb barrier the (^{3}He, α) yield from nickel was negligible in comparison with the yield from ^{18}O. However, the strong flux of elastically scattered ^{3}He ions, which, of course, could not be stopped in a foil without also stopping the α particles, made it impractical to use a solid-state detector to detect the α particles in order to study the ^{18}O(^{3}He, αn) reaction. Instead the magnetic spectrometer was used at 10°, which is at the peak of the $L = 1$ angular distribution leading to the $T = \frac{3}{2}$ level. Since the $T = \frac{3}{2}$ level has spin $\frac{1}{2}$, the angular distribution of the decay neutrons is isotropic in the center-of-mass system, regardless of the angle of detection of the α particles from the populating reaction.

A 140-μm-thick silicon surface-barrier counter was placed in the focal plane of the spectrometer and a time spectrum of neutrons emerging at 280° in coincidence with α particles from the ^{18}O(^{3}He, α)-^{17}O ($T = \frac{3}{2}$) reaction was accumulated by starting the TAC with the silicon detector and stopping it with the neutron counter. Time spectra were obtained from a coincidence run of 12-h duration with the magnet set on the ^{17}O ($T = \frac{3}{2}$) peak and two 5-h runs with the magnet set on the background on either side of the peak. A flat background of chance coincidences, determined from the average number of counts in the time spectrum with apparent flight times faster than γ rays, was subtracted from all three spectra. The two corrected background spectra were then normalized to the same charge as the spectrum taken on the peak and subtracted from it. The resultant spectrum is shown in Fig. 14.

The neutron detector was the same one employed at CIT for the ^{13}C decays, but for the ^{17}O measurement the slow channel threshold was lowered to $\frac{1}{10}$ of the midpoint of the Compton edge of ^{137}Cs γ rays. This change increased the detection efficiency for 0.8-MeV neutrons from the decay of the $T = \frac{3}{2}$ level of ^{17}O to the first and second excited states of ^{16}O. The detector was placed 52 cm from the target and was housed in a lead shield with a 5-cm wall thickness. The smooth curves shown in Fig. 14 are experimentally determined line shapes for monoenergetic neutrons of energies appropriate for the ^{17}O decays. Because of the sizable "tail" on the intense peak, arising from decays to the ground state of ^{16}O, it was necessary to measure the line shape for neutrons of this energy rather carefully, in order to determine the branching ratios, particularly for the weak branch to the excited states. The "tail" is caused by scattering of neutrons into the detector by the surrounding material (primarily the magnetic spectrometer and its relatively thick-walled scattering chamber), and its shape was found to depend upon the angular distribution of the emitted neutrons. Since the ^{17}O ($T = \frac{3}{2}$) decay distribution is isotropic except for a small center-of-mass correction, it was necessary to find a reaction which produced neutrons of approximately the correct energy, did not produce other neutron groups within 6 MeV of the primary group, and had an angular distribution which was as close as possible to isotropic. The ^{13}C(α, n) reaction at 4.70-MeV bombarding energy has a resonance which is nearly isotropic[44] and this reaction was used to determine the line shape for 6.8-MeV neutrons. A similar determination of the line shape for neutrons from the decays to the first two excited states of ^{16}O was made using the T(p, n) reaction at 1.7-MeV incident energy, which is also roughly isotropic. Absolute-detection efficiencies were found by comparing yields of the line-shape data to spectra taken with the standard detector geometry with the same targets and bombarding energies.

The branching ratios obtained are listed in Table II. The quoted errors are dominated by uncertainties in the detection efficiency and, for the excited state decays, an uncertainty in the background under the peak. No corrections for impurity groups or for unresolved levels of ^{17}O were deemed necessary because of the quality of the α-particle spectrum from the spectrometer.

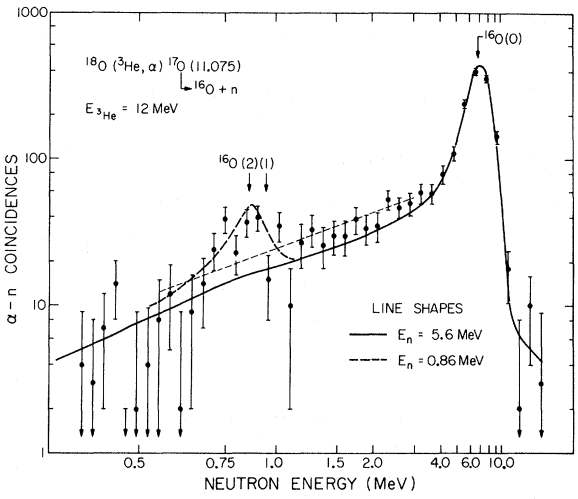

FIG. 14. Time-of-flight spectrum of neutrons in coincidence with α particles detected from the ^{18}O(^{3}He, α)^{17}O (11.075, $T = \frac{3}{2}$) reaction. A uniform chance-coincidence background and normalized real-coincidence background spectra have been subtracted. The solid curve is a line shape for 5.6-MeV neutrons, obtained from the ^{13}C(α, n)-^{16}O (0.0) reaction at an incident energy of 4.70 MeV; the darker dashed curve is a line shape for 0.86-MeV neutrons, obtained from the T(p, n) reaction at 1.7 MeV. The lighter dashed curve indicates the maximum background assumed in the calculation of the branching ratio for the decay of the ^{17}O($T = \frac{3}{2}$) level to ^{16}O (6.05 + 6.13).

4. EXPERIMENTAL CHECKS FROM THE MEASUREMENT OF KNOWN BRANCHING RATIOS

Because the technique used in our branching ratio measurements was fairly complex and involved sizable corrections for dead times, etc., we felt it was mandatory to measure some known branching ratios as a check. It was important to measure both neutron and proton decaying states, and to use both solid and gaseous targets. These requirements were met by obtaining branching ratios for the 6.86-MeV $J^\pi = \frac{5}{2}^+$ state of ^{13}C, and the unresolved 3.81-MeV ($J^\pi = 1^+$) and 3.91-MeV ($J^\pi = 0^-$) states[45] of ^{16}F. These states are expected to have branching ratios of unity since they have only one open particle-decay channel; the former decays by neutron emission to the ground state of ^{12}C and the latter two by proton emission to the ground states of ^{15}O.

The ^{13}C state was populated in the ^{11}B(^{3}He, p) reaction with the protons detected at 0°, using identical apparatus to that employed at CIT for the decays of the ^{13}C $T = \frac{3}{2}$ state. Sample singles and coincidence spectra are shown in Fig. 15. Since $J = \frac{5}{2}^+$ for the ^{13}C(6.86) level, the angular correlation should be of the form

$$dB/d\Omega(\theta) = A_0 + A_2 P_2(\cos\theta) + A_4 P_4(\cos\theta) .$$

The least-squares fit to the data of this expression is shown in Fig. 16(a). A branching ratio of 1.05 ± 0.11 was obtained for this decay. The decays of ^{16}F states were studied using the same apparatus as used for the ^{17}F decays; the levels were were populated by the ^{14}N(^{3}He, n)^{16}F reaction, and the neutrons were detected at 0°. Sample singles and coincidence spectra are shown in Fig. 17. As the spins of the 3.81- and 3.91-MeV levels are ≤ 1, the angular correlation for this case was fitted by an expression containing terms up to P_2. This fit is shown in Fig. 16(b). A branching ratio of 0.99 $\pm$ 0.09 was obtained for these decays. Since the measured branching ratios are unity within the experimental errors for these test cases, we conclude that our techniques, corrections, and error estimates are reliable.

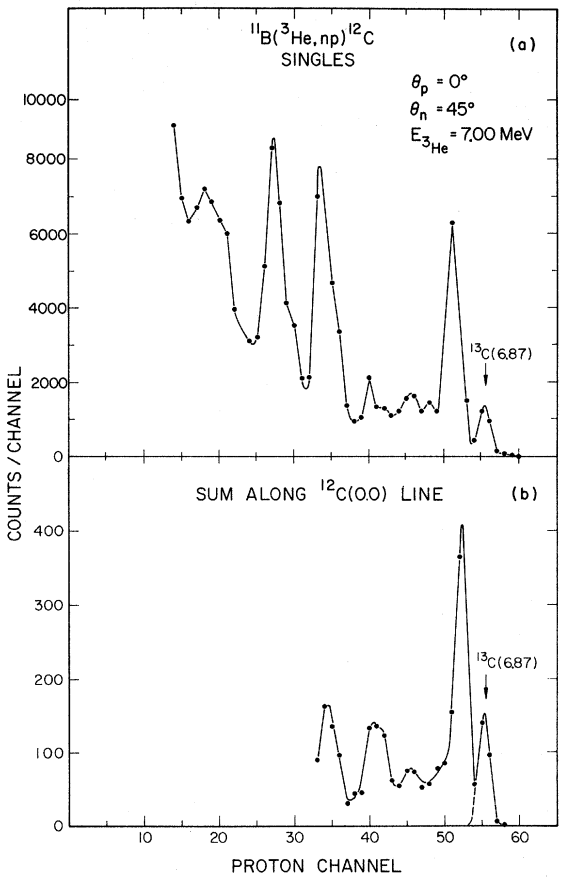

FIG. 15. (a) Charged-particle singles spectrum from the ^{11}B(^{3}He, p)^{13}C reaction showing the population of the ^{13}C (6.87) level. (b) Projection onto the proton-energy axis of the kinematic curve corresponding to the ^{11}B-(^{3}He, np)^{12}C (0.0) reaction.

5. INTERPRETATION OF THE BRANCHING-RATIO MEASUREMENTS

A. Isospin Mixing of the 15.1-MeV $T = \frac{3}{2}$ States in $A = 13$

The decay properties of the lowest $T = \frac{3}{2}$ levels of ^{13}N and ^{13}C are listed in Table I. The nucleon decay branching ratios are from this work. The radiative width of the ^{13}C level is from inelastic electron scattering studies.[21,22] The radiative width for the ^{13}N level is obtained by combining the observed resonance strength ($\Gamma_{p_0}\Gamma_{\gamma_0}/\Gamma$) from the ^{12}C($p, \gamma$) reaction[20] with our value for Γ_{p_0}/Γ. The total width of the ^{13}C level is obtained from resonance work,[34] but also independently from inelastic electron scattering[21] and γ-ray branching ratio measurements[28] [$\Gamma = (\Gamma_{\gamma_0}/\Gamma)^{-1}\Gamma_{\gamma_0}$]. The total width of the ^{13}N state is obtained from a combination of resonance[20] and branching ratio measurements,[28] $\Gamma = (\Gamma_{p_0}/\Gamma)^{-2}(\Gamma_{p_0}\Gamma_{\gamma_0}/\Gamma)(\Gamma_{\gamma_0}/\Gamma_{p_0})^{-1}$, and independently from elastic proton scattering.[27] The particle decay widths are obtained by multiplying our branching ratios by the adopted best value for the total width.

Two features of these decay widths are particularly striking:

(1) The equality of the isospin-allowed $\Delta T = 1$ radiative decay widths of ^{13}C and ^{13}N. The ratio of reduced transition probabilities: $B(M1)$ ^{13}N/$B(M1)$ ^{13}C = 1.02 ± 0.20.

(2) The strong asymmetry in the isospin-forbidden

particle widths and total widths of the $T=\frac{3}{2}$ levels.

The equality of the isospin-changing γ-ray transition strengths is easily understood. In first-order perturbation theory, i.e., negligible isospin mixing, the ratio of the transition probabilities is just

$$R=\left|\frac{\langle \frac{3}{2},+\frac{1}{2}|H_{\text{E.M.}}|\frac{1}{2},+\frac{1}{2}\rangle}{\langle \frac{3}{2},-\frac{1}{2}|H_{\text{E.M.}}|\frac{1}{2},-\frac{1}{2}\rangle}\right|^2,$$

where the states are labeled by T and T_z. The conventional radiation operator $H_{\text{E.M.}}$ is assumed to transform as electric charge and thus contains only isoscalar and isovector components. For $\Delta T=1$ radiation the isoscalar term cannot contribute and from the Wigner-Eckhart theorem we have

$$R=\left|\frac{(\frac{1}{2}+\frac{1}{2},10|\frac{3}{2}+\frac{1}{2})(\frac{3}{2}\|T_1^0\|\frac{1}{2})}{(\frac{1}{2}-\frac{1}{2},10|\frac{3}{2}-\frac{1}{2})(\frac{3}{2}\|T_1^0\|\frac{1}{2})}\right|^2=1.0$$

which is consistent with the experimental value. Isospin impurities will, of course, cause R to differ from unity but the effect is negligible since the impurities themselves are small. A detailed calculation of the isospin impurities[46] predicts a charge asymmetry of ~1% in the radiative widths which is much smaller than the experimental uncertainties in R. In Sec. 5 C we will consider the effects of a proposed isotensor E.M. current, which could cause R to differ from unity even in the case where isospin mixing can be ignored.

The marked asymmetry in isospin-forbidden nucleon decay widths can also be understood on a fairly simple basis. To interpret the asymmetries we must remove the trivial charge-dependent effects of differences in phase space and barrier penetration for protons and neutrons. Presumably we can account for such effects by dividing the branching ratios by the $l=1$ penetration factors (using $r=4.0$ fm) to obtain ratios of reduced widths,

$$\theta^2(0_1^+)/\theta^2(2_1^+)=\frac{\text{BR}(0_1^+)}{\text{BR}(2_1^+)}\,\frac{P(2_1^+)}{P(0_1^+)}.$$

In this case, division by penetration factors does not greatly affect the result and the large asymmetry is still present in the ratio of reduced widths (see Table I). We will try to understand the significance of the asymmetries by using lowest-order perturbation theory, mixing $T=\frac{1}{2}$ levels into the mass 13, $T=\frac{3}{2}$ states, and $T=1$ levels into the ^{12}C states. The symmetry of the γ decays supports the reasonableness of a perturbation approach. We ignore mixing of $T=2$ states in ^{12}C since the $T=2$ levels occur at excitation energies

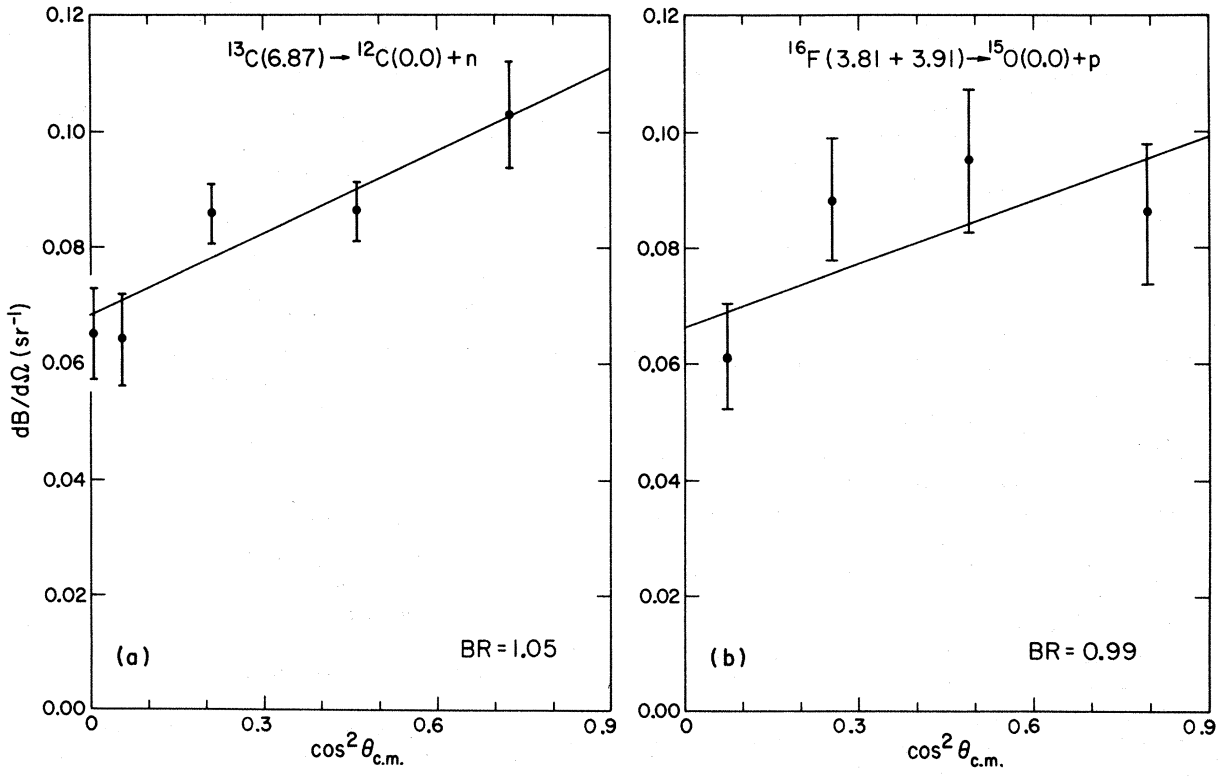

FIG. 16 (a), (b) Differential branching ratios for the neutron decay of the ^{13}C (6.87) level to the ground state of ^{12}C, and for the proton decay of the unresolved 3.81- and 3.91-MeV levels of ^{16}F to the ground state of ^{15}O.

above 27 MeV. The initial (mass 13, $T=\frac{3}{2}$) and final (^{12}C + nucleon) states may be written,

$$|i\rangle = |a_k;\ T=\tfrac{3}{2},\ T_z\rangle + \sum_j \beta_j(T_z)|b_j;\ T=\tfrac{1}{2},\ T_z\rangle,$$

$$|f\rangle = \{|c_k;\ T=0,0\rangle + \sum_j \delta_j|d_j;\ T=1,0\rangle\}|\ T=\tfrac{1}{2},\ T_z\rangle,$$

where the sums run over all possible admixed states. For the case with $T_z=\pm\frac{1}{2}$

$$\langle f|i\rangle = \sum_j \beta_j(T_z)\langle c|b_j\rangle + (\tfrac{2}{3})^{1/2}\sum_j \delta_j^*\langle d_j|a\rangle \pm \Theta(\beta\delta).$$

The terms $\langle c|b_j\rangle$ and $\langle d_j|a\rangle$ are equal to $\sqrt{N}\times\mathrm{CFP}(i\to f)$, where N is the number of active nucleons and CFP is the appropriate coefficient of fractional parentage. We assume there are no fortuitous cancellations in first order and neglect terms of order $\beta\delta$ and higher. Then the ratio of reduced widths to final states c and c' becomes

$$\frac{\theta_c^{\,2}}{\theta_{c'}^{\,2}} = \left|\frac{\langle f|i\rangle}{\langle f'|i\rangle}\right|^2 = \left|\frac{\sum_j \beta_j(T_z)\langle c|b_j\rangle + (\tfrac{2}{3})^{1/2}\sum_j \delta_j^*\langle d_j|a\rangle}{\sum_j \beta_j(T_z)\langle c'|b_j\rangle + (\tfrac{2}{3})^{1/2}\sum_j \delta_j^*\langle d_j'|a\rangle}\right|^2,$$

where $\beta_j(T_z)$ is given by

$$\beta_j(T_z) = (E_a - E_{b_j})^{-1}\langle b_j T_z|H_{\mathrm{NC}}|aT_z\rangle.$$

H_{NC} is an isospin nonconserving two-body interaction, such as the Coulomb force, which contains only isoscalar, isovector, and isotensor terms, $H_{\mathrm{NC}} = T_0^0 + T_1^0 + T_2^0$, and E_a and E_{b_i} are zeroth-order (charge-independent) excitation energies. The T_z dependence of β_j is given by the Wigner-Eckhart theorem

$$\beta_j(T_z=\pm\tfrac{1}{2}) = -(E_a - E_{b_j})^{-1}[(3)^{-1/2}A_j^{\,1} \pm (5)^{-1/2}A_j^{\,2}],$$

where $A_j^{\,1}$ and $A_j^{\,2}$ are reduced isovector and isotensor matrix elements of H_{NC}.

From the above expression for $\theta_c^{\,2}/\theta_{c'}^{\,2}$ we can immediately see that the large asymmetry in the ratio of reduced widths implies that:

(1) Isospin mixing in the mass 13 levels is important; i.e., isospin impurities in ^{12}C alone cannot cause an asymmetry. If the β_j all vanish, then $\theta_c^{\,2}/\theta_{c'}^{\,2}$ is independent of T_z.

(2) A strong isotensor impurity in the mass 13 levels is required. Purely isovector impurities in mass 13 and in ^{12}C cannot produce asymmetries in ratios of reduced widths, since δ_j^* is independent of T_z and the isovector component of $\beta_j(T_z)$ is the same for $T_z=+\frac{1}{2}$ and $T_z=-\frac{1}{2}$.

(3) The isotensor amplitude in the mass-13 states must be comparable with the isovector amplitude plus the term due to $T=1$ impurities in ^{12}C. The isotensor amplitude changes sign when $T_z\to -T_z$, while the term due to impurities in ^{12}C and the isovector amplitude do not. To get a strong asymmetry, cancellation must occur, so these terms must be of the same order.

Isospin impurities in the ground and first excited states of ^{12}C are probably smaller than the impurities in the mass-13 $T=\frac{3}{2}$ levels. In ^{12}C the nearest $T=1$ state that could mix into the ground state lies at least 17.8 MeV away. If, in fact, we can neglect the impurities in ^{12}C, the asymmetries in reduced widths imply that:

(4) More than one $T=\frac{1}{2}$ state is substantially involved in the mixing of the mass-13 $T=\frac{3}{2}$ levels. If the δ_j^* are negligible for all j and only one β_j is significantly greater than zero, then the ratio of reduced widths becomes $|\langle c|b_k\rangle/\langle c'|b_k\rangle|^2$, which is independent of T_z and only a property of the admixed state b_k. Probably the admixtures in both ^{13}C and ^{13}N are complex and not dominated by a single state. However, in principle the impurity in each nucleus could be dominated by a single

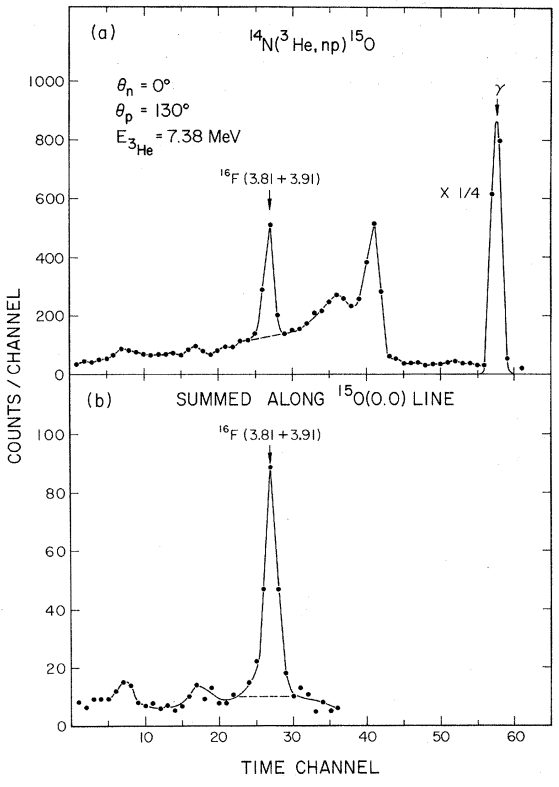

FIG. 17. (a) Neutron time-of-flight spectrum from the ^{14}N(^{3}He,n)^{16}F reaction showing the population of the ^{16}F (3.81 + 3.91) levels. (b) Projection onto the neutron time-of-flight axis of the kinematic curve corresponding to the ^{14}N(^{3}He,np)^{15}O (0.0) reaction.

state, as long as it was a *different* state in ^{13}C and ^{13}N.

(5) The isotensor amplitude in the mass-13 states must be comparable to the isovector amplitude.

Since our results contradict the usual assumption that off-diagonal isotensor amplitudes are small compared with isovector amplitudes, it is instructive to consider in a qualitative fashion, the source of the large isotensor term. We recall that any one-body model of the isospin-nonconserving interaction implicitly neglects isotensor mixing. However, the isospin-violating interaction is actually a two-body operator; in particular for the Coulomb force, it is a two-body operator that vanishes unless both of the particles are charged. For the sake of discussion we shall consider pure $1p$-shell zeroth-order wave functions for the $J^\pi = \frac{3}{2}^-$, $T = \frac{3}{2}$, and $T = \frac{1}{2}$ states. In this model, the ^{13}C states have 2 proton holes and 1 neutron hole in the $1p$ shell, and the ^{13}N states have 1 proton hole and 2 neutron holes. The isospin-mixing matrix elements for mass 13 will have the form

$$\langle C(\mathrm{hhh})_{T=1/2} | H_C | C(\mathrm{hhh})_{T=3/2} \rangle ,$$

where H_C is the Coulomb potential and C denotes the closed core. This can be expanded into a sum of two-body matrix elements of three kinds; one where H_C operates only on the holes, one where H_C operates only on the core particles, and one where H_C connects core particles and holes. The last two kinds of terms vanish identically by orthogonality. Terms of the first kind also vanish in ^{13}N (which has only one proton hole) but are present in ^{13}C (which has two charged holes). Hence, in this simple model, ^{13}N has no $1p$-shell isospin impurities induced by the two-body Coulomb force while ^{13}C does (see for example Ref. 47). Since we showed above that T_z-dependent isospin impurities implied a strong isotensor mixing, we can understand how a strong isotensor matirx element can arise from even the simplest microscopic model of the nuclear states.

It is interesting to note that the mass-13 decays may be particularly sensitive to the charge-dependent nuclear force. If this force is predominantly the result of the mass difference of the charged and neutral pions it will be largely charge symmetric and have an isotensor character. It will therefore give equal contributions in ^{13}C and ^{13}N, in direct contrast to the Coulomb force which mixes $1p$-shell states only in ^{13}C.

Let us consider the isospin-forbidden branching ratios predicted by the extreme single-particle shell model. In this picture the low-lying $\frac{3}{2}^-$ states in mass 13 have a $p_{3/2}^{-1}p_{1/2}^{-2}$ configuration; we assume that the isospin impurity in the ^{13}C 15.11-

TABLE III. Some properties of $J^\pi = \frac{3}{2}^-$, $T = \frac{1}{2}$ levels in mass 13 (Ref. a).

E_x (MeV)	Γ (keV)	$\Lambda(M1)$ (W.u.)	^{13}B logft	BR(0^+)	BR(2^+)
			^{13}C		
3.684	$(4.0 \pm 0.35) \times 10^{-4}$ [c]	0.38	4.45 ± 0.05 [b]	0.0	0.0
(9.499) [d]	≤ 5		...	...	...
9.899	28	0.16 [c]	...	1.0 ± 0.2 [e]	<0.15 [e]
11.72	125 ± 30	~ 0.1 [c]	...	0.67 ± 0.16 [e]	0.33 ± 0.08 [e]
(13.76) [f]	≈ 350				
			^{13}N		
3.509	63 ± 5	0.68	4.52 ± 0.13 [g]	1.00	0.0
9.52	30	...	5.18 ± 0.14 [g]	0.6 ± 0.1 [h]	0.4 ± 0.1 [h]
11.87	130	...	...		

[a] Unless otherwise noted, taken from Ref. 32.

[b] K. W. Jones, W. R. Harris, M. T. McEllistrem, and D. E. Alburger, Phys. Rev. 186, 978 (1969).

[c] Reference 21.

[d] This level is not firmly established as having $J^\pi = \frac{3}{2}^-$.

[e] Present work.

[f] This level is seen strongly in inelastic electron scattering but its spin is not determined.

[g] J. E. Esterl, J. C. Hardy, R. G. Sextro, and J. Cerny, Phys. Letters 33B, 287 (1970).

[h] J. E. Esterl, J. C. Hardy, R. G. Sextro, and J. Cerny, Phys. Letters 33B, 287 (1970); A. C. L. Barnard, J. B. Swint, and T. B. Clegg, Nucl. Phys. 86, 130 (1966); E. M. Bernstein, J. J. Ramirez, R. E. Shamu, Pui-Wah Chang, and M. Soga, Phys. Rev. Letters 28, 293 (1972) find that for the decay of this level to the 2^+ state of ^{12}C $\Gamma_{j=1/2}/\Gamma_{j=3/2} > 0.9$.

MeV $T=\frac{3}{2}$ level will have the same configuration. This impurity can decay to $p_{3/2}{}^{-2}p_{1/2}{}^{-2}$ or to $p_{3/2}{}^{-1}p_{1/2}{}^{-3}$ by emission of a $p_{3/2}$ or $p_{1/2}$ neutron, respectively, but cannot decay to the ^{12}C ground state which in this extreme model is $p_{1/2}{}^{-4}$. On the other hand, decay to the 4.44-MeV state ($p_{3/2}{}^{-1}p_{1/2}{}^{-3}$) is possible. We would thus expect from this model that the strongest branching ratio measured in this work would be the ^{13}C decay to ^{12}C(4.43), all the other decays would arise from processes we have neglected, such as configuration mixing, higher-order terms in the perturbation expansion, excitation out of the $1p$ shell, impurities in ^{12}C, direct mixing, and the charge-dependent nuclear force. It is interesting that the mixing induced by impurities in ^{12}C (assumed to be only $T=1$) and excitation out of the $1p$ shell (assuming it is dominated by the one-body Coulomb potential) have a pure isovector character and hence will give equal contributions to the decay amplitudes in ^{13}C and ^{13}N. From Table I we see that, in fact, the strongest observed branching ratio is $^{13}\mathrm{C}(T=\frac{3}{2})\rightarrow{}^{12}\mathrm{C}(4.43)+n$, which is ~4 times stronger than the ^{13}N branches and $^{13}\mathrm{C}(T=\frac{3}{2})\rightarrow{}^{12}\mathrm{C}(0.0)+n$. The decay widths of the $T=\frac{3}{2}$ levels in ^{13}N and ^{13}C to the 7.6-MeV 0^+ state of ^{12}C are particularly interesting. These decays are presumably governed by that portion of the isospin impurity which has (sd) shell components, since the 7.6-MeV state of ^{12}C is probably not a p-shell state (Cohen and Kurath's[46] 0_2^+ state lies at an excitation energy of 13.5 MeV). The observed widths are small and roughly the same size in ^{13}C and ^{13}N, which supports our simple picture.

In order to do a realistic calculation of the isospin-forbidden particle widths of the $\frac{3}{2}^-$, $T=\frac{3}{2}$ levels, one has to know the properties of the $\frac{3}{2}^-$, $T=\frac{1}{2}$ levels, their excitation energies, coefficients of fractional parentage, and off-diagonal charge-dependent matrix elements. We summarize what is known about the positions of these $\frac{3}{2}^-$ levels in Fig. 18, where the experimentally determined negative-parity levels as well as the charge-independent calculations of Cohen and Kurath[48] (CK) are displayed. In Table III some of the properties of the $J^\pi=\frac{3}{2}^-$, $T=\frac{1}{2}$ levels are given. Our knowledge of these levels is quite meager. The lowest $\frac{3}{2}^-$ levels in ^{13}N and ^{13}C have been identified, but the spectroscopic factor for the ^{13}C level ($S=0.22$) deduced from the $^{12}\mathrm{C}(d,p)$ reaction[49] differs by a factor of 7 from the reduced width for the analog

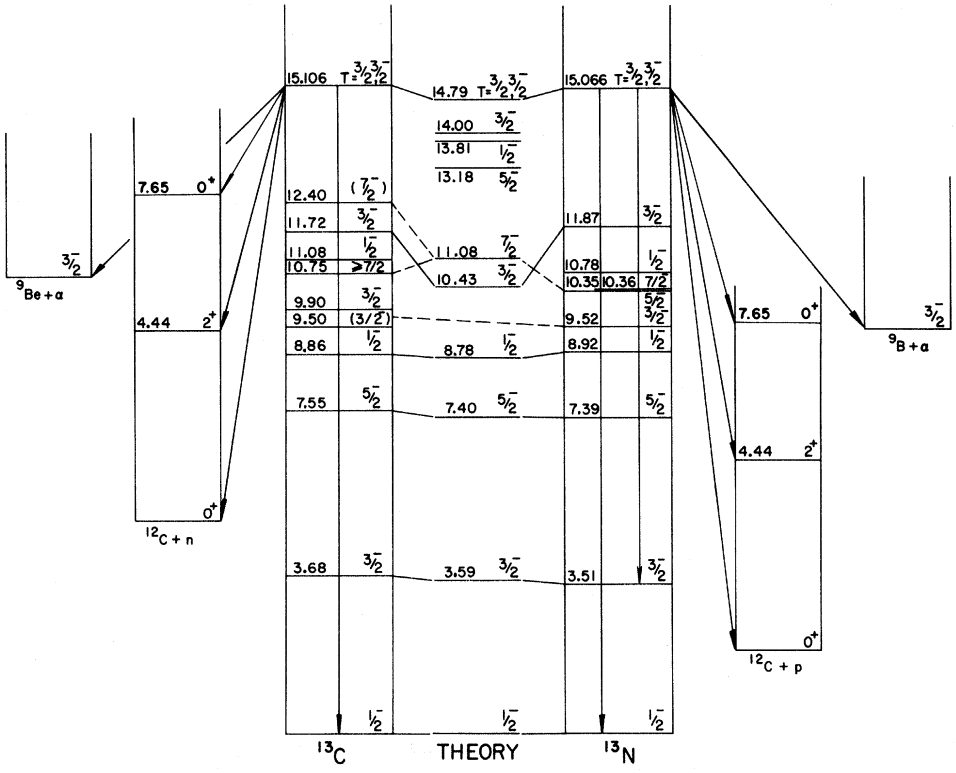

FIG. 18. Partial-energy-level diagram for ^{13}C and ^{13}N. Experimental numbers are from Ref. 32. Theoretical numbers are from Ref. 48.

level in $^{13}N(\theta_p^2 = 0.031)$ obtained from the $^{12}C(p,p)$ reaction.[32] One or possibly two $\frac{3}{2}^-$ levels occur at an excitation energy of ~9.5 MeV and a state has been seen at ~11.8 MeV. CK predict p-shell $\frac{3}{2}^-$, $T = \frac{1}{2}$ levels to lie at excitation energies of 3.59, 10.43, 14.00, 17.45, and 19.84 MeV. Only for the lowest level of CK can one unambiguously identify the calculated states with experimentally determined levels. On the basis of two-particle pickup reactions[50] and inelastic electron scattering,[21] the 11.8-MeV levels are associated with the 10.43-MeV level of CK. The 9.5-MeV levels are apparently not accounted for in the CK calculations. No state corresponding to the 14.00-MeV level of CK has been observed. This is especially vexing since a $T = \frac{1}{2}$ level in this vicinity might be expected to play an important role in the isospin mixing if the energy denominator were sufficiently small.

A detailed calculation[47] of the isospin-forbidden widths in mass 13 has been performed by Arima and Yoshida (AY) who used the CK wave functions for the charge-independent basis. They find that there are two important sources of the impurities induced by the Coulomb force: the mixing of the $1p$-shell states in ^{13}C, and the mixing of continuum states (levels above the $1p$ shell) which is approximately charge symmetric and gives nearly equal contributions in ^{13}C and ^{13}N. We have neglected this last type of mixing in our discussion above. AY did find that the decay widths are quite sensitive to a charge-dependent (isotensor) nuclear force, although it is not needed to obtain agreement with experiment. Their results are quite sensitive to the exchange character of the charge-independent nuclear force used in calculating the widths and to the exact location of CK's third $\frac{3}{2}^-$, $T = \frac{1}{2}$ state, which plays a very important role in the isospin mixing because of its small energy denominator (0.8 MeV). With suitable choice of the exchange character and a small change in the position of this state they obtain excellent qualitative agreement with our results as can be seen in Table IV. Even the relative amounts of $j = \frac{1}{2}$ and $j = \frac{3}{2}$ which we obtain in the decay $^{13}N^* \rightarrow {}^{12}C(2^+) + p$ are in rough agreement with the calculation. Unfortunately the relative amounts of $j = \frac{1}{2}$ and $j = \frac{3}{2}$ could not be determined for the corresponding ^{13}C decay. The calculated $j = \frac{1}{2}$ fraction is quite sensitive to the assumed 14.00-MeV state of CK and a measurement of this fraction would constitute a good test of the theory. It would also be valuable to demonstrate that the choice of nuclear-force parameters that produces reasonable values for the isospin-forbidden widths also gives the correct widths for the isospin-allowed decay widths of the $T = \frac{1}{2}$ states, such as the 11.7-MeV level in ^{13}C. The apparent charge asymmetry in the reduced widths of the 3.6-MeV states is presumably due to inconsistent analyses.

The pioneering calculation of AY represents an important contribution to our understanding of the detailed mechanism of isospin mixing. However the quantitative results depend strongly upon shell-model calculations (in particular upon the location

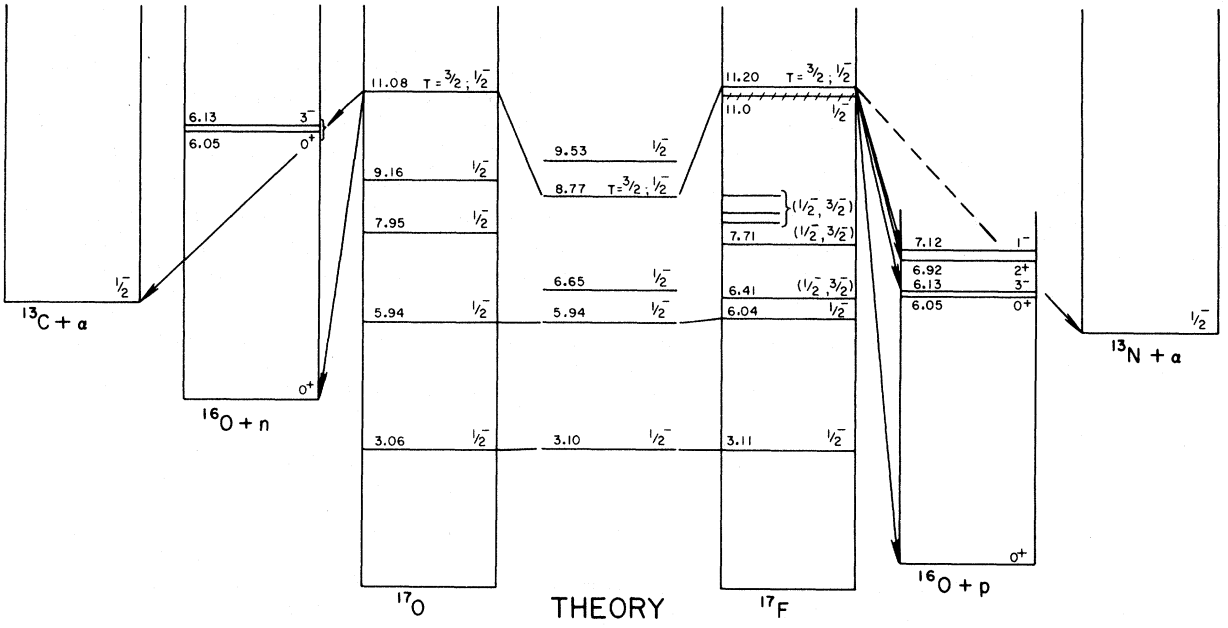

FIG. 19. Energy-level diagram showing positions of known or possible $\frac{1}{2}^-$ levels in ^{17}O and ^{17}F (see Table V). Theoretical numbers are from Ref. 51.

and properties of an as yet unobserved level calculated to lie 0.8 MeV below the lowest $T=\frac{3}{2}$ state). Because of the sensitivity of the calculation by AY to the unobserved shell-model state, it is instructive to estimate the decay widths in ^{13}C from a simple model where the entire width comes from the mixing of the "antianalog" state at 3.5 MeV, which which should have a large Coulomb matrix element. With a Coulomb matrix element of 110 keV (CK predict 165 keV) and CK's spectroscopic factors, assuming that $\Gamma=2P\theta^2$, where

$$\theta^2=S\theta_{\mathrm{WL}}{}^2\left|\frac{\langle T=\frac{3}{2}|H_c|T=\frac{1}{2}\rangle}{E_{3/2}-E_{1/2}}\right|^2,$$

$\theta_{\mathrm{WL}}{}^2$ is the Wigner limit width, S is the spectroscopic factor, and P is an $l=1$ penetration factor evaluated at $R=4.0$ fm, we obtain $\Gamma_{n_0}=0.34$ keV and $\Gamma_{n_2}=1.42$ keV. This compares well with the experimental values 0.35 ± 0.10 and 1.31 ± 0.24. The agreement is somewhat fortuitous since many additional coherent contributions have been neglected. However, it suggests that two-body Coulomb mixing within the p shell can contribute a large part of the isospin impurity for ^{13}C, even if no unobserved $J^\pi=\frac{3}{2}^-$ level lies particularly near the $T=\frac{3}{2}$ state. Since shell-model wave functions and energies are not reliable for such highly excited states, a really credible calculation of isospin mixing must employ experimentally determined level parameters. A strong effort to identify the $\frac{3}{2}^-$ $T=\frac{1}{2}$ levels and to measure their reduced widths is needed for a better understanding of isospin mixing in mass 13.

B. Isospin Mixing in the 11-MeV $T=\frac{3}{2}$ States in $A=17$

The decay properties of the lowest $T=\frac{3}{2}$ levels of ^{17}O and ^{17}F are listed in Table II. The nucleon decay branching ratios are from this work and Ref. 8. The total width of the ^{17}F level is obtained by combining an inelastic scattering measurement[38] of Γ_{p_0}/Γ_0 [i.e., $\Gamma=\Gamma_{p_0}(\Gamma_{p_0}/\Gamma)^{-1}$]. The width of the ^{17}O level is found by observing it as a resonance in the ^{13}C(α,n_0) reaction.[42] The asymmetry observed in the particle decays is even more striking than that observed for mass 13. The decay width of ^{17}O$(T=\frac{3}{2})$ to the ^{16}O ground state is nearly 100 times greater than the corresponding width in ^{17}F. Again we attempt to remove the uninteresting effects of charge-dependent differences in phase space barrier penetrations by dividing the branching ratios by penetration factors to obtain ratios of reduced widths. We assume for the moment that the ^{17}O decays go to the 3^- member of the 6-MeV doublet in ^{16}O as is the case for ^{17}F. (Decays to the 0_2^+ state would involve an obvious charge asymmetry.) A strong asymmetry remains in the reduced widths. However, in this case the Q values for ^{17}F and ^{17}O decays to the excited states of ^{16}O are sufficiently different that division by penetration factors constitute a significant correction. Although the penetrabilities are quite sensitive to the radius parameter used in the calculation, the variation with radius is similar for the mirror decays. The ratio of the penetrability for an ^{17}O decay to that for the analogous ^{17}F decay varies by less than 30% for radii between 3.5 and 5.0 fm. Thus in the comparison of ratios of reduced widths in ^{17}F and ^{17}O, the uncertainty due to the choice of nuclear radius (a radius of 4.4 fm was employed) is smaller than the experimental errors in the ^{17}O case. We may conclude that in mass 17, as well as in mass 13, more than one state is mixed into the $T=\frac{3}{2}$ level and that the isovector and isotensor admixtures have comparable intensities.

Again, as in mass 13, we turn to an extreme single-particle model to understand in a qualitative fashion the possible sources of the asymmetric decays. In this case the configuration of the $T=\frac{3}{2}$ and $T=\frac{1}{2}$, $J^\pi=\frac{1}{2}^-$ states will be 2p-1h structures built on a closed 1p shell. Detailed calculations[51] using this limited basis have been fairly successful, which supports this simple model. Isospin mixing between 2p-1h states in mass 17

TABLE IV. Comparison of measured decay widths of the 15.1-MeV $T=\frac{3}{2}$ levels of ^{13}C and ^{13}N with shell-model calculation (Ref. a).

	^{13}C			^{13}N			
	Γ_{n_0} (keV)	Γ_{n_1} (keV)	$\Gamma_{\gamma_0}^{M1}$ [b] (eV)	Γ_{p_0} (keV)	Γ_{p_1} (keV)	$\langle 2\|\|1/2\|\|3/2\rangle / \langle 2\|\|3/2\|\|3/2\rangle$	$\Gamma_{\gamma_0}^{M1}$ [b] (eV)
Expt	0.35 ± 0.10	1.31 ± 0.24	22.7 ± 2.6	0.19 ± 0.05	0.12 ± 0.03	2.1 ± 2.4	23.0 ± 3.6
Theory	0.19	1.65	28.35	0.25	0.14	$3.32\exp(-0.1i)$	28.13

[a] The calculations of Γ_{n_0}, Γ_{n_1}, Γ_{p_0}, and Γ_{p_1} are given in Table 9 of Ref. 47. A Rosenfeld force has been used with a range of 1.414 fm. The energy separation of the nearest $\frac{3}{2}^-$, $T=\frac{1}{2}$ state is increased by 50% over the value predicted by CK.

[b] The theoretical values of $\Gamma_{\gamma_0}(M1)$ are from Ref. 46.

has been discussed by Walker and Schlobohm.[52] Denoting holes by superscript bars, the 2p-1h configurations of ^{17}O and ^{17}F may be written

^{17}O: $\nu\pi\bar{\pi}+\nu\nu\bar{\nu}$,

^{17}F: $\pi\pi\bar{\pi}+\pi\nu\bar{\nu}$,

where π and ν denote protons and neutrons, respectively. The Coulomb matrix elements $\langle C(\mathrm{pph})_{T=1/2}|H_C|C(\mathrm{pph})_{T=3/2}\rangle$ can be decomposed into two-body particle-particle and particle-hole terms. For the $T=\frac{1}{2}$ states the particles can be coupled to $T_{\mathrm{part}}=0$ or $T_{\mathrm{part}}=1$. The particle-particle Coulomb matrix elements vanish unless both particles are protons and as a result are nonzero only for $T_{\mathrm{part}}=1$ states in ^{17}F. Now let us consider the particle-hole Coulomb matrix elements. These vanish for the case where the hole is a neutron. Thus in ^{17}F the $T_{\mathrm{part}}=0$ configurations cannot be mixed into the $T=\frac{3}{2}$ level by the particle-hole Coulomb force while in ^{17}O they can. As was the case in mass 13, even the simplest microscopic model can, in principle, produce asymmetric decays and hence comparable isotensor and isovector Coulomb matrix elements.

A realistic calculation of the mixing must employ measured properties of the admixed states. In Table V and Fig. 19 we show some properties of known or possible $J^\pi=\frac{1}{2}^-$, $T=\frac{1}{2}$ levels in ^{17}O and ^{17}F. In Ref. 51 four $\frac{1}{2}^-$ states are predicted to lie at less than 10 MeV. The experimental data are quite incomplete above an excitation energy of 6 MeV. However, a $\frac{1}{2}^-$ state in ^{17}F has been identified[53] at an excitation energy of 11.00 MeV ($\Gamma\simeq 0.4$ MeV). Because of its proximity to the 11.20-MeV $T=\frac{3}{2}$ level, this $T=\frac{1}{2}$ state may play an important role in the mixing. The $T=\frac{1}{2}$ state has $\Gamma_{p_0}/\Gamma\approx 0.1$ which could mean that it dominates the decays of ^{17}F, since the $T=\frac{3}{2}$ level has $\Gamma_p/\Gamma\approx 0.09$. As yet there is no explanation for the most remarkable feature of the mass-17 decays – that the decay width of the $T=\frac{3}{2}$ level in ^{17}O to the ground state of ^{16}O is $\simeq$100 times greater than the corresponding width in ^{17}F.

C. Radiative Widths of the Lowest $T=\frac{3}{2}$ Level of ^{13}C and ^{13}N and the Proposed Isotensor Electromagnetic Current

It is usually assumed that the E.M. transition operator transforms like the charge and contains only isoscalar and isovector components. In this case first-order perturbation theory predicts that the reduced transition probabilities for the $\Delta T=1$ radiative decays of the lowest $T=\frac{3}{2}$ levels of ^{13}C and ^{13}N should be in the ratio $R_{13}=B(M1)^{13}\mathrm{N}/B(M1)^{13}\mathrm{C}=1$. However, there is at present no compelling evidence either in nuclear or particle physics, for restricting the E.M. field to isoscalar and isovector components.[54,55] In fact, recent analyses by Sanda and Shaw[23] and Berardo *et al.*[24] of analogous pion photoproduction reactions in the $\Delta(1236)$ $T=\frac{3}{2}$ resonance region ($\gamma+p\to\Delta^+\to\pi^++n$ and $\gamma+n\to\Delta^0\to\pi^-+p$) find support for an appreciable isotensor current. In the absence of isotensor currents the radiative widths of the Δ^+ and Δ^0 should be in the ratio

$$R_\Delta=\frac{\Gamma(\Delta^+\to p+\gamma)}{\Gamma(\Delta^0\to n+\gamma)}=1.$$

TABLE V. Some properties of possible $J^\pi=\frac{1}{2}^-$, $T=\frac{1}{2}$ levels in mass 17 (Ref. a).

^{17}O				^{17}F					
E_x (MeV)	Γ (keV)	logft [b]	J^π	E_x (MeV)	Γ (keV)	logft [b, c]	Γ_{p_0}/Γ	$\Gamma_{p_1}/\Gamma_{p_0}$	J^π
3.055		6.9±0.1	$\frac{1}{2}^-$	3.105	19±1	6.44±0.61	1.0		$\frac{1}{2}^-$
5.935	23±10		$\frac{1}{2}^-$	6.036	28	4.42±0.01	1.0		$\frac{1}{2}^-$
				6.406 [c]		5.80±0.13	1.0		$(\frac{1}{2}^-,\frac{3}{2}^-)$
				7.708 [c]		5.67±0.12		<5	$(\frac{1}{2}^-,\frac{3}{2}^-)$
7.947	79±10		$\frac{1}{2}^-$	8.075 [c]		3.96±0.01		0.49±0.02	$(\frac{1}{2}^-,\frac{3}{2}^-)$
				8.436 [c]		3.85±0.02		6.0 ±0.5	$(\frac{1}{2}^-,\frac{3}{2}^-)$
				8.825 [c]		4.23±0.02		8.2 ±1.2	$(\frac{1}{2}^-,\frac{3}{2}^-)$
9.16	4±3		$\frac{1}{2}^-$						
				11.00 [d]	≈400		≈0.10	...	$\frac{1}{2}^-$

[a] Unless otherwise noted, taken from F. Ajzenberg-Selove, Nucl. Phys. A166, 1 (1971).
[b] logft for ^{17}N or ^{17}Ne β decays.
[c] Reference 8.
[d] Reference 53.

Upon examining the differences in total cross sections

$$\delta = \sigma_t(\gamma + n \to \pi^- + p) - \sigma_t(\gamma + p \to \pi^+ + n)$$

as a function of energy, Sanda and Shaw find effects they cannot ascribe to kinematics. They attribute the discrepancy to an isotensor current, which would permit the Δ^+ and Δ^0 to have different radiative widths since in this case

$$R_\Delta = \left| \frac{1-\chi_\Delta}{1+\chi_\Delta} \right|^2 ,$$

where $\chi_\Delta = (\frac{3}{5})^{1/2} A_2^\Delta / A_1^\Delta$ and A_1^Δ and A_2^Δ are reduced isovector and isotensor amplitudes of the E.M. interaction. Berardo *et al.* have analyzed their $\pi^- + p \to n + \gamma$ data and existing photoproduction cross sections using the Sanda-Shaw model. They obtain acceptable fits for

$$-0.52 \leq \frac{A_2^\Delta}{A_1^\Delta} \leq -0.13 .$$

If isotensor currents do exist then $\Delta T = 1$, *nuclear* transitions will also, at some level of accuracy, show departures from charge symmetry.[25] In nuclei, isotensor amplitudes are suppressed, since a "$\Delta T = 2$" photon cannot couple to a single nucleon which has $T = \frac{1}{2}$. But the current can couple, for example, to virtual $\Delta(1236)$ $T = \frac{3}{2}$ baryons formed in the process $N + N \to \Delta + \Delta$ within nucleus. Consequently the ratio[25]

$$R_{13} = \frac{B(M1)(^{13}\mathrm{N}^* \to {}^{13}\mathrm{N} + \gamma)}{B(M1)(^{13}\mathrm{C}^* \to {}^{13}\mathrm{C} + \gamma)} = \left[1 - 4\left(\frac{3}{5}\right)^{1/2} \frac{A_2^{13}}{A_1^{13}} \right]$$

should show a small departure from unity if a sizable isotensor amplitude were present in the Δ decays as suggested by the analysis of Ref. 24.

It will clearly be difficult to separate the effects of "$\Delta T = 2$" photons from ordinary isospin impurities if the two effects are of the same size. In mass 13 the calculated charge asymmetries arising from isospin impurities[46] are between $\approx 1\%$ and $\approx 3.5\%$. A rough upper limit of $|A_2/A_1| \lesssim 0.036$ has been estimated[56] for the effects on nuclear transitions of an isotensor component in $\Delta \to N + \gamma$ of the size indicated by Berardo *et al.*[24] This would produce an asymmetry of $\leq 11\%$. A careful measurement of the radiative widths is therefore of considerable interest. From the present experimental value $R_{13} = 1.02 \pm 0.20$ an upper limit $|A_2^{13}/A_1^{13}| < 0.07$ can be inferred. While this is still too large to place really useful limits on isotensor effects, the experimental uncertainties could be significantly improved. At present the error in R_{13} is dominated by the $^{12}\mathrm{C}(p, \gamma_0)$ measurement,[20] which has a quoted uncertainty of $\pm 14.5\%$. This could be significantly improved with a new measurement.

Let us briefly discuss other possible nuclear tests for isotensor currents. In addition to the comparison of *absolute* radiative widths mentioned above, one could search for asymmetries in the *relative* widths of two sets of analogous $\Delta T = 1$ transitions (i.e., a charge dependence of relative γ-ray branching ratios), or for transitions between states which differ by two units of isospin. The comparison of analogous branching ratios is inherently quite precise. However, isotensor amplitudes will produce charge asymmetries only if the appropriate matrix elements have opposite signs (see Ref. 56). The best upper limit for $T = 2 \to T = 0$ γ-ray transitions[10] yields a much weaker limit on possible isotensor currents than the present measurement, since in the case studied the $\Delta T = 2$ transition is $E2$ while the $\Delta T = 1$ transition is $M1$.

There is an additional incentive for comparisons of the type reported here. The apparent asymmetry in the $\Delta(1236)$ decays was most pronounced in a comparison of the reactions

$$p + \gamma \to \Delta^+ ,$$

$$\Delta^0 \to \pi^- + p .$$

There have been suggestions that the isotensor currents may involve time-reversal violations as well.[57] In that case, one should probably compare nuclear reactions which are also time-reversal analogs. The mass-13 decays have precisely this form. In the $^{13}\mathrm{N}$ case the width is measured for the radiative *decay* $^{13}\mathrm{N}^* \to {}^{13}\mathrm{N} + \gamma$, while in $^{13}\mathrm{C}$ the width is measured for *excitation* by inelastic electron scattering $^{13}\mathrm{C} + \gamma \to {}^{13}\mathrm{C}^*$. Furthermore these $M1$ transitions are strong, which reduces the influence of small isospin impurities which would play a significant role is highly retarded decays.

D. Conclusions

The particle decays of $T = \frac{3}{2}$ levels in the mirror nuclei $^{13}\mathrm{C}$, $^{13}\mathrm{N}$ and $^{17}\mathrm{O}$, $^{17}\mathrm{F}$ show strong charge asymmetries, indicating that the isovector and isotensor mixing amplitudes have similar magnitudes. This conclusion is consistent with the observed decays of $T = 2$ states in the $2s$-$1d$ shell where $\Delta T = 2$ α-particle emission competes successfully with isospin-forbidden proton decay. Strong charge asymmetries arise naturally from a shell-model description of the nuclear states. Unfortunately, detailed calculations of the mixing must rely upon theoretical estimates of the properties of the high-lying admixed states, since experimental data on these levels are not available. At this point a most useful avenue for further work

lies in locating the $T=\frac{1}{2}$ states that may be admixed, and measuring their partial decay widths. As the $T=\frac{1}{2}$ level spectra in $A=13$ and $A=17$ become better understood, one may be able to learn more about the mechanisms of isospin mixing and ultimately about the charge dependence of the nucleon-nucleon force itself.

ACKNOWLEDGMENTS

We would like to acknowledge the stimulating atmosphere of the Kellogg Radiation Laboratory where this work was begun and of Chalk River Nuclear Laboratories where later work was performed. Even the long and difficult coincidence runs were a great pleasure in this enviroment. E.G.A. thanks Professor G. T. Garvey for several discussions on the physics of isospin mixing and we all acknowledge the interest and encouragement of Professor C. A. Barnes who initially suggested the comparison of the decay widths of the $T=\frac{3}{2}$ analog states. We are grateful to Professor S. Yoshida for communicating his results to us prior to publication. We thank T. K. Alexander, O. Häusser, and J. C. Hardy for their assistance in the work at Chalk River.

APPENDIX

To understand the reaction kinematics of our experiments let us consider the case of mass 13 in some detail.

The lowest $T=\frac{3}{2}$ level of ^{13}N was produced in the ^{11}B(^{3}He, n) reaction which preferentially populates the $T=\frac{3}{2}$ state. The branching ratios were obtained by detecting the decay proton in coincidence with the neutron populating the decaying state. In this case the reaction of interest is $^3\mathrm{He}+{}^{11}\mathrm{B}\rightarrow n+p+{}^{12}\mathrm{C}$ which proceeds sequentially through a resonance in the $p+{}^{12}$C system corresponding to the lowest $T=\frac{3}{2}$ level of ^{13}N. The kinematics for the three body reaction ^{11}B(^{3}He, np)^{12}C are shown in Fig. 3. For fixed angles of the neutron and proton detectors, the particle energies are constrained to lie on "kinematic curves," one for each state of ^{12}C. A resonance in the $p+{}^{12}$C system will appear as an enhancement in the density of events lying on the appropriate kinematic curve at the point were the invariant mass of the $p+{}^{12}$C system has the resonant value. These should occur at the interaction of the "kinematic curves" with the horizontal lines drawn on the figure for various excited states of ^{13}N. However, by charge symmetry there are essentially as many resonances in the $n+{}^{12}$C system as in $p+{}^{12}$C and these also produce enhancements on the kinematic curves at intersections with the vertical lines drawn for various excited states of ^{13}C. To distinguish an enhancement caused by a resonance in the $p+{}^{12}$C system from one due to the $n+{}^{12}$C system, one can show that the invariant mass in the $p+{}^{12}$C system corresponds to a known resonance in ^{13}N and that there exists no resonance in ^{13}C that could also produce the enhancement. Alternatively, one can vary the incident energy or detector angle and find in which system the enhancement has a constant invariant mass. We have in most cases used the latter method to identify resonances, since it is completely unambiguous and is not dependent upon the energy resolution and calibration of the detectors. For completeness we should mention that, in principle, one must also consider resonances in the system of the two light particles (in the present case $p+n$). However, no sharp resonances exist in this system and such effects can be neglected in our experiments.

The angular correlation between the particle populating an unstable state with $j>\frac{1}{2}$, and the nucleon emitted in its decay is not, in general, isotropic. Hence in order to measure a branching ratio one must integrate decay measurements performed over the entire sphere. To simplify this integration we have detected the particle populating the decaying level at 0°, in which case the apparatus for producing the state (beam, collimators, and detector) is symmetric about the beam (z) axis. Thus j_z is conserved and the density matrix for the decaying state is diagonal. Furthermore, $j_z=S_z^i+S_z^t-S_z^0$ where S_z^i, S_z^t, and S_z^0 refer to the spins of the incident, target, and outgoing light particles, respectively. The target and beam are unpolarized and by parity conservation the outgoing particle cannot have any longitudinal polarization. Therefore, the density matrix must have the property that its diagonal element corresponding to $j_z=+m$ is equal to the element corresponding to $j_z=-m$, and the decaying state is said to be aligned.

A general expression for the angular correlation may be written as

$$\frac{dB}{d\Omega}(\theta,\phi)=\sum\rho_{k\kappa}(aa')\epsilon_{k_b\kappa_b}(bb')\epsilon^*_{k_L\kappa_L}(LL')\times(k_b\kappa_b k_L\kappa_L|k\kappa)\hat{a}\hat{a}'\hat{k}_b\hat{k}_L\begin{Bmatrix} b & L & a\\ b' & L' & a'\\ k_b & k_L & k\end{Bmatrix}\times\langle b|L\|a\rangle\langle b'|L'\|a\rangle^*, \quad (2)$$

where the summation is over $aa'bb'LL'k\kappa k_b\kappa_b k_L\kappa_L$ and $\hat{a}\equiv(2a+1)^{1/2}$. This is equation 2.93 of Ferguson's[58] book on angular correlations and we follow his formalism. The initial ($\vec{a}$) and final ($\vec{b}$) states are related by the vector addition formula $\vec{a}=\vec{b}+\vec{L}$. $\rho_{k\kappa}(aa')$ is a statistical tensor describing

the initial state as produced by the populating reaction and may be written in terms of a density matrix constructed using the eigenfunctions $|a\alpha\rangle$ of the spin of the initial state, thus

$$\rho_{k\kappa}(aa') = \sum_{\alpha\alpha'}(-)^{a'-\alpha'}(a\alpha, a'-\alpha'|k\kappa)\langle a\alpha|\rho|a'\alpha'\rangle .$$

For an aligned state, where the density matrix satisfies

$$\langle a\alpha|\rho|a'\alpha'\rangle = \delta_{aa'}\delta_{\alpha\alpha'}\langle a-\alpha|\rho|a-\alpha\rangle ,$$

we must have $\kappa = 0$ and $k =$ even $\leq 2a$. This may be seen from the following:

$$(-)^{a-\alpha}(a\alpha, a-\alpha|k0) = (-)^{2a-k-2\alpha} \times [(-)^{a+\alpha}(a-\alpha, a\alpha|k0)]$$

$$= (-)^{k}[(-)^{a+\alpha}(a-\alpha, a\alpha|k0)] .$$

Therefore terms with opposite signs for α cancel if $k =$ odd, so $\rho_{k_0}(aa) = 0$ for k odd. If the recoiling nucleus is not detected and the detector of the emitted particle is axially symmetric, then

$$\epsilon k^{*}_{\kappa_b}(bb')\epsilon^{*}_{k_L\kappa_L}(LL') = \text{const}\, Y^{K}_{k}(\theta, \phi)\delta_{k_b0}\delta_{\kappa_b0},$$

and the angular correlation may therefore be written

$$\frac{dB}{d\Omega}(\theta) = \sum_{\substack{L=0 \\ L=\text{even}}}^{L=2a} A_L P_L(\cos\theta),$$

which considerably simpilfies the integration over solid angle. For the lowest $T = \frac{3}{2}$ level of ^{13}C and ^{13}N, $a^{\pi} = \frac{3}{2}^{-}$ and so $W(\theta) = A_0 + A_2 P_2(\cos\theta)$.

For the lowest $T = \frac{3}{2}$ level of ^{17}O and ^{17}F, $a^{\pi} = \frac{1}{2}^{-}$, and the angular correlation is isotropic regardless of the polarization of the state (i.e., regardless of the angle of the detector that observes the reaction populating the state) as long as the state has definite parity. Referring to Eq. (2), we may select the z axis in the direction of polarization of the state, so that we have axial symmetry and $\kappa = 0$. As we do not detect the recoiling nucleus with spin b, we have $k_b = \kappa_b = 0$, hence $k = k_L$ and $\kappa_L = \kappa = 0$. The efficiency tensor $\epsilon^{*}_{k_L\kappa_L}(LL')$ now contains the Clebsch-Gordan coefficient $(l0, l'0|k0)$ which vanishes unless $l + l' + k =$ even, where $L = l + s$ for the emitted particle. Conservation of parity requires $l + l'$ even and so k is even, but $k \leq 1$ and so $k = 0$ and the angular correlation is isotropic.

The angular correlation will also be isotropic if the initial state is unpolarized, regardless of its spin and parity. This situation can occur in our experiments if the double-stripping reactions populating the $T = \frac{3}{2}$ states in ^{13}N and ^{13}C proceed by means of a simple, one-step direct reaction and transfer a $T = 1$, $S = 0$, $L = 0$ dinucleon to an unpolarized target. If, however, there is a significant compound nuclear contribution to the reaction, we can expect to observe nonzero A_2 terms for the angular correlation of the nuclear decays of the $\frac{3}{2}^{-}$ levels of ^{13}C and ^{13}N. In this case we can separate the reduced matrix elements for decay by emission of a $p_{1/2}$ or $p_{3/2}$ particles. For the decay of the $\frac{3}{2}^{-}$, $T = \frac{3}{2}$ level to the 0^{+} ground state of ^{12}C, only $p_{3/2}$ emission is possible and the ratio A_2/A_0 is sufficient to determine the ratio of alignment parameters ρ_{20}/ρ_{00}. For the decay to the 2^{+}, 4.43-MeV level of ^{12}C, both $p_{1/2}$ and $p_{3/2}$ are allowed. Then

$$\frac{dB}{d\Omega}(\theta) \alpha \sum_{kLL'} \rho_{k0}(10, 10|k0)W(11, LL'; k\tfrac{1}{2}) \times W(L\tfrac{3}{2}L'\tfrac{3}{2}; 2k)\langle 2|L\|\tfrac{3}{2}\rangle\langle 2|L'\|\tfrac{3}{2}\rangle^{*},$$

where $k = 0, 2$ and $L, L' = \frac{1}{2}, \frac{3}{2}$. Since the ρ_{k0} are determined from the ratio A_2/A_0 from the decay to the ground state, we have

$$\left(\frac{A_2}{A_0}\right)_{4.43} = \left(\frac{A_2}{A_0}\right)_{0.0} \times (-0.6) \times \left\{\frac{1.33\,\mathrm{Re}(\langle 2|\tfrac{1}{2}\|\tfrac{3}{2}\rangle\langle 2|\tfrac{3}{2}\|\tfrac{3}{2}\rangle^{*}) + |\langle 2|\tfrac{3}{2}\|\tfrac{3}{2}\rangle|^2}{|\langle 2|\tfrac{1}{2}\|\tfrac{3}{2}\rangle|^2 + |\langle 2|\tfrac{3}{2}\|\tfrac{3}{2}\rangle|^2}\right\}.$$

Unlike E.M. matrix elements, the relative phases of the reduced matrix elements for particle emission with different L values are not uniquely defined. However, the two reduced matrix elements corresponding to $L = l + \frac{1}{2}$ and $L = l - \frac{1}{2}$ generally have relative phase near 0 or 180°, since the Coulomb and angular momentum barriers which dominate the decaying wave function depend only on l and not on L. This is supported by the detailed calculations of AY[47] who find that in all cases the relative phase of the reduced matrix elelents for $p_{1/2}$ and $p_{3/2}$ are within 6° of 0° or 180°.

If one assumes that

$$\langle 2\|\tfrac{1}{2}\|\tfrac{3}{2}\rangle = Ce^{i\phi}\langle 2\|\tfrac{3}{2}\|\tfrac{3}{2}\rangle$$

and that $\phi = 0$, then

$$\left(\frac{A_2}{A_0}\right)_{4.43} = \left(\frac{A_2}{A_0}\right)_{0.0}(-0.6)\left(\frac{1.33C+1}{1+C^2}\right).$$

For decay to the 0^{+}, 7.65-MeV level of ^{12}C, only $p_{3/2}$ emission is possible and so the ratio of A_2/A_0 is defined only by the alignment parameters. It should therefore be identical to the A_2/A_0 ratio observed for decay to the 0^{+} ground state.

*Work supported in part by the National Science Foundation Grant No. GP-28027.

†Present address: Physics Department, University of Washington, Seattle, Washington 98195.

‡Present address: Nuclear Physics Branch, AECL, Chalk River Nuclear Laboratories, Chalk River, Ontario, Canada KOH 1JO.

§Present address: Physics Department, Kansas State University, Manhattan, Kansas 66502.

¶Present address: Physics Department, University of Texas, Austin, Texas 78712.

‖Present address: Physics Department, India Institute of Technology, Kanpur, V. P., India.

**Present address: Tel-Aviv University, Tel-Aviv, Israel.

[1]R. J. Blin-Stoyle, *Selected Topics in Nuclear Spectroscopy* (North-Holland, Amsterdam, 1964), p. 213.

[2]S. D. Bloom, in *Isobaric Spin in Nuclear Physics*, edited by J. D. Fox and D. Robson (Academic, New York, 1966), p. 123 and references therein.

[3]D. H. Wilkinson, in *Nuclear Spectroscopy B*, edited by F. Ajzenberg-Selove (Academic, New York, 1960), p. 852.

[4]E. K. Warburton, in *Isobaric Spin in Nuclear Physics* (see Ref. 2), p. 90; E. K. Warburton and J. Weneser, in *Isospin in Nuclear Physics*, edited by D. H. Wilkinson (North-Holland, Amsterdam, 1969), p. 173.

[5]C. P. Browne, in *Isobaric Spin in Nuclear Physics* (see Ref. 2), p. 136.

[6]L. Meyer-Schützmeister, D. von Ehrenstein, and R. G. Allas, Phys. Rev. 147, 743 (1966).

[7]R. Bloch, R. E. Pixley, and P. Truöl, Phys. Letters 25B, 215 (1967).

[8]J. C. Hardy, J. E. Esterl, R. G. Sextro, and J. Cerny, Phys. Rev. C 3, 700 (1971).

[9]S. J. Skorka, J. Hertel, and T. W. Retz-Schmidt, Nucl. Data A2, 347 (1966).

[10]K. A. Snover, Ph.D. thesis, Stanford University, 1969 (unpublished); K. A. Snover, D. W. Heikkinen, F. Riess, H. M. Kuan, and S. S. Hanna, Phys. Rev. Letters 22, 239 (1969); S. S. Hanna, in *Isospin in Nuclear Physics* (seeRef. 4), p. 591.

[11]R. L. McGrath, J. Cerny, J. C. Hardy, G. Goth, and A. Arima, Phys. Rev. C 1, 184 (1970).

[12]J. Jänecke, in *Isospin in Nuclear Physics* (see Ref. 4), p. 297.

[13]K. T. Hecht, Nucl. Phys. A102, 11 (1967); A114, 280 (1968).

[14]G. F. Bertsch, Phys. Rev. 174, 1313 (1968).

[15]J. C. Hardy, H. Brunnader, J. Cerny, and J. Jänecke, Phys. Rev. 183, 854 (1969).

[16]W. M. MacDonald, in *Nuclear Spectroscopy B* (see Ref. 3), p. 932; W. M. MacDonald, Phys. Rev. 100, 51 (1955); 101, 271 (1956); 110, 1420 (1958).

[17]J. M. Soper, in *Isospin in Nuclear Physics* (see Ref. 4), p. 229.

[18]J. Jänecke, Nucl. Phys. A128, 632 (1969).

[19]E. M. Henley, in *Isospin in Nuclear Physics* (see Ref. 4), p. 15.

[20]F. S. Dietrich, M. Suffert, A. V. Nero, and S. S. Hanna, Phys. Rev. 168, 1169 (1969).

[21]G. Wittwer, H. G. Clerc, and G. A. Beer, Phys. Letters 30B, 634 (1969).

[22]G. A. Peterson, Phys. Letters 25B, 549 (1967).

[23]A. I. Sanda and G. Shaw, Phys. Rev. Letters 24, 1310 (1970); Phys. Rev. D 3, 243 (1971).

[24]P. A. Berardo, R. P. Haddock, J. Helland, B. M. K. Nefkins, L. J. Verhey, M. E. Zeller, A. S. L. Parsons, and P. Truoel, Phys. Rev. Letters 26, 205 (1971); and R. P. Haddock, private communication.

[25]R. J. Blin-Stoyle, Phys. Rev. Letters 23, 535 (1969).

[26]J. Cerny, Ann. Rev. Nucl. Sci. 18, 27 (1968).

[27]M. J. LeVine and P. D. Parker, Phys. Rev. 186, 1021 (1969). We have corrected the width quoted here for the 15.07-MeV state by assuming that the resonance anomaly is proportional to $(\Gamma_{p_0}/\Gamma)\Gamma$.

[28]C. L. Cocke, J. C. Adloff, and P. Chevallier, Phys. Rev. 176, 1120 (1968).

[29]E. G. Adelberger, A. B. McDonald, and C. A. Barnes, Nucl. Phys. A124, 49 (1969).

[30]E. G. Adelberger and A. B. McDonald, Nucl. Phys. A145, 497 (1970).

[31]I. S. Sherman, R. G. Roddick, and A. J. Metz, IEEE Trans. Nucl. Sci. NS-15 (No. 3), 500 (1968).

[32]F. Ajzenberg-Selove, Nucl. Phys. A152, 1 (1970).

[33]D. C. Hensley, Ph.D. thesis, California Institute of Technology, 1969 (unpublished), and private communication; D. C. Hensley and C. A. Barnes, Bull. Am. Phys. Soc. 10, 1194 (1965).

[34]K. A. Snover, E. G. Adelberger, and F. Riess, Bull. Am. Phys. Soc. 13, 883 (1968); and unpublished data.

[35]A. B. McDonald, Ph.D. thesis, California Institute of Technology, 1969 (unpublished).

[36]J. E. Brolley and J. L. Fowler, in *Fast Neutron Physics*, edited by J. B. Marion and J. L. Fowler (Interscience, New York, 1960), Part I, Chap. 1c.

[37]M. D. Goldberg, J. D. Anderson, H. P. Stoering, and C. Wong, Phys. Rev. 122, 1510 (1961).

[38]J. R. Patterson, H. Winkler, and C. S. Zaidens, Phys. Rev. 163, 1051 (1967). We have corrected the upper limit on the width of the 11.20-MeV state given in this paper for the more precise value for Γ_p/Γ obtained in the present work.

[39]G. M. Temmer, in *Nuclear Isospin*, edited by J. D. Anderson, S. D. Bloom, J. Cerny, and W. W. True (Academic, New York, 1969), p. 81.

[40]C. A. Barnes, E. G. Adelberger, D. C. Hensley, and A. B. McDonald, in *International Nuclear Physics Conference*, edited by R. L. Becker, C. D. Goodman, P. N. Stelson, and A. Zucker (Academic, New York,1967), p. 884, and D. C. Hensley, Ph.D. thesis, California Institute of Technology, 1969 (unpublished).

[41]C. Detraz and H. H. Duhm, Phys. Letters 29B, 29 (1969).

[42]A. B. McDonald, T. K. Alexander, and O. Häusser, Bull. Am. Phys. Soc. 16, 489 (1971).

[43]R. H. Spear, J. D. Larson, and J. D. Pearson, Nucl. Phys. 41, 353 (1963).

[44]J. M. Morris, Ph.D. thesis, Australian National Unibersity, Canberra, 1967 (unpublished).

[45]E. G. Adelberger and A. V. Nero, unpublished data.

[46]H. Sato and S. Yoshida, Bull. Am. Phys. Soc. 16, 601 (1971).

[47]A. Arima and S. Yoshida, Nucl. Phys. A161, 492 (1971); and S. Yoshida, private communication.

[48]S. Cohen and D. Kurath, Nucl. Phys. 73, 1 (1965); A101, 1 (1967).

[49]J. P. Schiffer, G. C. Morrison, R. H. Siemssen, and

B. Zeidman, Phys. Rev. 164, 1274 (1967).
[50]D. G. Fleming, J. Cerny, C. C. Maples, and N. K. Glendenning, Phys. Rev. 166, 1012 (1968).
[51]B. Margolis and N. de Takacsy, Can. J. Phys. 44, 1431 (1966).
[52]G. E. Walker and D. Schlobohm, Nucl. Phys. A140, 49 (1970).
[53]H. R. Hiddleston, J. Aymar, and S. E. Darden, Bull. Am. Phys. Soc. 16, 489 (1971); and H. R. Hiddleston, private communication.
[54]N. Dombey and P. K. Kabir, Phys. Rev. Letters 17, 730 (1966).
[55]S. L. Adler, Phys. Rev. Letters 18, 519 (1967).
[56]E. G. Adelberger and D. P. Balamuth, Phys. Rev. Letters 27, 1597 (1971).
[57]A. I. Sanda and G. Shaw, Phys. Rev. Letters 26, 1087 (1971).
[58]A. J. Ferguson, *Angular Correlation Methods in Gamma Ray Spectroscopy* (North-Holland, Amsterdam, 1965).

PHYSICAL REVIEW C VOLUME 7, NUMBER 3 MARCH 1973

Spin and Spin-Isospin Symmetry Energy of Nuclear Matter

J. Dabrowski
Institute for Nuclear Research, Warsaw, Poland
and
P. Haensel
Institute for Theoretical Physics, Warsaw University, Warsaw, Poland
(Received 13 September 1972)

The expression, $E/A=\epsilon_{\rm vol}+\frac{1}{2}\epsilon_\tau\alpha_\tau^2+\frac{1}{2}\epsilon_\sigma(\alpha_n+\alpha_p)^2+\frac{1}{2}\epsilon_{\sigma\tau}(\alpha_n-\alpha_p)^2$, for the ground-state energy of nuclear matter with an excess of neutrons, of spin-up neutrons, and of spin-up protons (characterized by the corresponding parameters, $\alpha_\tau=(N-Z)/A$, $\alpha_n=(N_\uparrow-N_\downarrow)/A$, and $\alpha_p=(Z_\uparrow-Z_\downarrow)/A$), contains three symmetry energies: the isospin symmetry energy ϵ_τ, the spin symmetry energy ϵ_σ, and the spin-isospin symmetry energy $\epsilon_{\sigma\tau}$. General expressions for ϵ_σ and $\epsilon_{\sigma\tau}$ are obtained in terms of the K matrix which depends on four different Fermi momenta. With suitable approximations, numerical values of ϵ_σ and $\epsilon_{\sigma\tau}$ (and also of ϵ_τ) are derived using the Brueckner-Gammel-Thaler, the Hamada-Johnston, and the Reid soft-core nucleon-nucleon potentials. The most reliable results, obtained with the Reid soft-core potential, are: $\epsilon_\tau=61$ MeV, $\epsilon_\sigma=74$ MeV, and $\epsilon_{\sigma\tau}=73$ MeV. The possibility of estimating the energies of the spin and spin-isospin modes of collective nuclear excitations is discussed.

I. INTRODUCTION

Let us consider nuclear matter composed of $N_\uparrow$ neutrons with spin up, $N_\downarrow$ neutrons with spin down, $Z_\uparrow$ protons with spin up, and $Z_\downarrow$ protons with spin down. All the nucleons are contained in a periodicity box of volume Ω. The composition of the system may be characterized by $A=N_\uparrow+N_\downarrow+Z_\uparrow+Z_\downarrow$, the neutron-excess parameter

$$\alpha_\tau=(N_\uparrow+N_\downarrow-Z_\uparrow-Z_\downarrow)/A=(N-Z)/A,$$

the neutron-spin-up-excess parameter $\alpha_n=(N_\uparrow-N_\downarrow)/A$, and the proton-spin-up-excess parameter $\alpha_p=(Z_\uparrow-Z_\downarrow)/A$.

The ground-state energy E of the system is subject to two conditions:

$$E(A,\alpha_\tau,\alpha_n,\alpha_p)=E(A,-\alpha_\tau,\alpha_p,\alpha_n), \quad (1)$$

$$E(A,\alpha_\tau,\alpha_n,\alpha_p)=E(A,\alpha_\tau,-\alpha_n,-\alpha_p). \quad (2)$$

The first one results from the charge independence of nuclear forces, and the second one from the time-reversal invariance of the interaction (or, in other words, from the requirement that E does not change when the spins of all the nucleons are reversed).

Because of these two conditions the expansion of E in powers of α_τ, α_n, and α_p takes the form

$$E/A=\epsilon_{\rm vol}+\tfrac{1}{2}\epsilon_\tau\alpha_\tau^2+\tfrac{1}{2}\epsilon_\sigma(\alpha_n+\alpha_p)^2+\tfrac{1}{2}\epsilon_{\sigma\tau}(\alpha_n-\alpha_p)^2, \quad (3)$$

where powers higher than quadratic are neglected. In expression (3), apart from the volume energy, $\epsilon_{\rm vol}$, and the usual (isospin) symmetry energy, denoted here by ϵ_τ, we have two more quantities: ϵ_σ and $\epsilon_{\sigma\tau}$. Quantity ϵ_σ is the measure of additional energy necessary to maintain a spin excess in the system, characterized by the spin-excess parameter, $\alpha_\sigma=\alpha_n+\alpha_p=(N_\uparrow+Z_\uparrow-N_\downarrow-Z_\downarrow)/A$. Quantity ϵ_σ is referred to further as the spin symmetry energy. Quantity $\epsilon_{\sigma\tau}$ is the measure of additional energy necessary to maintain in the system an excess of spin-up neutrons and spin-